Universidad de Huelva

DEPARTAMENTO DE QUÍMICA
Y CIENCIA DE LOS MATERIALES
PROFESOR J. C. VÍLCHEZ MARTÍN

Daniel Alejandro Sánchez-Rodas Navarro, catedrático del Departamento de Química "Prof. José Carlos Vílchez Martín", en relación a los criterios de calidad de la tesis doctoral "Contribución de fuentes de material particulado atmosférico en zonas industriales complejas", realizada por la doctoranda María Millán Martínez, y de la que soy codirector,

Informa

Que la tesis doctoral se ha completado con éxito, en referencia a los objetivos planteados y los resultados obtenidos, dando lugar a tres publicaciones científicas indexadas en Journal Citation Reports (JCR) en los cuartiles Q1:

Artículo 1. Source contribution and origin of PM10 and arsenic in a complex industrial region (Huelva, SW Spain). Publicado en Environmental Pollution. Factor de impacto 8.071. Cuartil Q1. Categoría: Environmental Sciences

Artículo 2. Contribution of anthropogenic and natural sources in PM10 during North African dust events in Southern Europe. Publicado en Environmental Pollution. Factor de impacto 8.071. Cuartil Q1. Categoría: Environmental Sciences

Artículo 3. Impact of the SARS-CoV-2 lockdown measures in Southern Spain on PM10 trace elements concentrations. Publicado en Chemosphere. Factor de impacto 7.086. Cuartil Q1. Categoría: Environmental Sciences

Fdo.

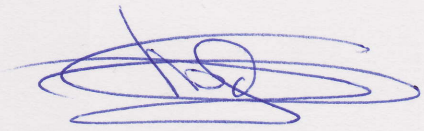

Daniel A. Sánchez-Rodas Navarro

Environmental Pollution 274 (2021) 116268

Contents lists available at ScienceDirect

Environmental Pollution

journal homepage: www.elsevier.com/locate/envpol

Source contribution and origin of PM10 and arsenic in a complex industrial region (Huelva, SW Spain)☆

María Millán-Martínez [a, b, *], Daniel Sánchez-Rodas [a, b], A.M. Sánchez de la Campa [a, c], Andrés Alastuey [d], Xavier Querol [d], Jesús D. de la Rosa [a, e]

[a] Associate Unit CSIC-University of Huelva "Atmospheric Pollution", Center for Research in Sustainable Chemistry - CIQSO, University of Huelva, E21071 Huelva, Spain
[b] Department of Chemistry, Faculty of Experimental Sciences, University of Huelva, Campus El Carmen s/n, 21071 Huelva, Spain
[c] Department of Mining, Mechanic, Energetic and Construction Engineering, ETSI, University of Huelva, 21071 Huelva, Spain
[d] Institute for Environmental Assessment and Water Research (IDÆA-CSIC), C/Jordi Girona 18-24, Barcelona 08034, Spain
[e] Department of Earth Science, Faculty of Experimental Sciences, University of Huelva, Campus El Carmen s/n, 21071 Huelva, Spain

ARTICLE INFO

Article history:
Received 16 July 2020
Received in revised form
10 November 2020
Accepted 8 December 2020
Available online 16 December 2020

Keywords:
Complex industrial area
Sulfide material
PM10
Pollutant gases
Arsenic speciation

ABSTRACT

Air pollution coming from industrial activities is a matter of interest since their emissions can seriously affect to the human health of nearby populations. A more detailed study about industrial emissions is required in order to discriminate different activities contributing to pollutant sources. In this sense, gaseous pollutants (NO_2, SO_2 and O_3) and PM10 levels has been studied in a complex industrial area in the southwest of Spain (La Rabida and the nearby city of Huelva) during the period 1996–2017. Hourly, daily, monthly and annual variations of PM10 and gaseous pollutants concentrations point to the industrial activity as the main SO_2 source. Furthermore, traffic and resuspension emissions contribute to the NO_2 and PM10 levels, respectively. Results from chemical composition of PM10 at both sites during the period 2015–2017 are characterized by high concentrations of the crustal components derived from natural and local resuspension. Arsenic is found to be the main geochemical anomaly at La Rabida (annual mean of 7 ng m^{-3}), exceeding the European annual target of 6 ng m^{-3}, which supposes a risk for the nearby population. An emission source from Cu-smelter has been identified in La Rabida and Huelva. A second source corresponding to emissions from polymetallic sulfides handling in a port area has been described for the first time in La Rabida. In addition, arsenic speciation results have identified three different As impacts scenarios as a function of the dominant wind direction, the SO_2 episodes and the As extraction efficiency: impact of the Cu-smelter, impact of the bulk polymetallic sulfides and a mixed impact of both sources.

1. Introduction

Atmospheric aerosol, also referred as Particulate Matter (PM), is a main pollutant in air characterized by the wide physico-chemical variety of its components and sources (Moreno et al., 2006; Giere and Querol, 2010; Calvo et al., 2013). With the aim of identifying PM origins, different source contribution models have been applied (e.g. Principal Component Analysis or Positive Matrix Factorization; Viana et al., 2008a,b; Belis et al., 2011; Hopke, 2016). These techniques enable the identification and quantification of natural sources (e.g. soils resuspension, desert dust or sea salt aerosols) and anthropogenic sources mainly related to exhaust and non-exhaust traffic (Amato et al., 2009), industrial (Viana et al., 2008b) and biomass burning emissions (Sánchez de la Campa et al., 2018).

Nowadays, most part of the world population is concentrated in urban areas, frequently located near industrial estates. Therefore, it is of high interest to quantify industrial sources apportionment, since their emissions can add toxic elements and compounds to atmospheric pollution, leading to a negative impact on human health (Pope, 2007). Sometimes, source contribution analysis are not able to discriminate different industrial activities because the corresponding studies are undertaken in urban areas. In this sense,

☆ This paper has been recommended for acceptance by Prof. Pavlos Kassomenos.
* Corresponding author. Associate Unit CSIC-University of Huelva "Atmospheric Pollution", Center for Research in Sustainable Chemistry - CIQSO, University of Huelva, E21071 Huelva, Spain.
E-mail address: maria.millan@dqcm.uhu.es (M. Millán-Martínez).

https://doi.org/10.1016/j.envpol.2020.116268
0269-7491/

industrial emissions can be mixed between them or with other urban sources such as traffic or local dust resuspension (Lee et al., 2003; Pandolfi et al., 2011; Fernández-Camacho et al., 2012). An exhaustive identification of sources contribution analysis is required in order to isolate the different industrial emissions and their quantification, and to compare with the results from a nearby urban area. In addition, it must be taken into account the impact of economic crisis on the atmospheric emissions in industrialized and developing countries, like the global recession starting in 2008 (Cusack et al., 2012; Monteiro et al., 2018; Li et al., 2018).

The urban area of Huelva (SW Spain) is a good example of a city influenced by complex industrial emissions (Querol et al., 2002; Alastuey et al., 2006). Trace elements such as Ni and V and pollutant gases (SO_2 and NO_x) have been studied in relation to petrochemical activities (Fernández-Camacho et al., 2012). Also, high concentrations of As and other toxic trace elements (Sb, Cu, Zn, Pb and Sn) in PM have been found in the city of Huelva (urban background) as a result of the emissions of a Cu smelter (González Castanedo et al., 2014; Chen et al., 2016). However, no source contribution studies have been undertaken within the industrial area in order to better discriminate emission sources.

The purpose of the present work is to identify the sources contribution of PM10 (coarse fraction of PM with aerodynamic diameter < 10 μm) in La Rabida (SW Spain), a monitoring stations near an industrial complex area. Furthermore, data obtained from the nearby urban station in the city of Huelva will be also considered to compare the impact of the industrial emissions at both sites. To this aim, pollutant gases and PM10 levels temporal series (1996–2017) were evaluated according to the wind direction in order to discriminate possible emission sources. Moreover, source apportionment analysis of the chemical composition and As speciation of PM10 samples (period 2015–2017), were carried out as a tool to distinguish between different industrial sources.

2. Methodology

2.1. Study area

The city of Huelva (145.000 inhabitants) is located in the SW of Spain, 5 km from the confluence of the Odiel and Tinto Rivers, which form the estuary of Huelva (Fig. 1). The province of Huelva, situated at the western end of the Guadalquivir River basin, has a Mediterranean climate with Atlantic influence. Winters are mild, with an annual mean temperature above 10 °C, and summers are warm with a mean temperature of 25 °C in the region, exceeding sometimes 40 °C. Precipitation is moderate (235 L m^{-2} in 2019) and occurs largely in winters since summers are dry (7 L m^{-2} between June–September 2019). Data were obtained from a station of the Spanish State Meteorological Agency (AEMET, 2019) located in Huelva. The wind direction is dominated mainly by two components due to the Atlantic breeze (SW) and the topography of the area: NW (Odiel River), and to a minor extent by NE (Tinto River) (see wind rose in Fig. 1). Daily air masses origin affecting to the study area were obtained using back trajectories provided by NOAA Air Resources Laboratory's (ARL) HYSPLIT model (Stein et al., 2015).

Air quality in the city of Huelva has been deeply studied because of its high industrialization since 1960's. The major industrial estates are settled down in two main areas at the S of the city (Fig. 1): Punta del Sebo and Nuevo Puerto. A petrochemical industry and other industrial activities such as TiO_2 production are developed at the Nuevo Puerto estate. The production of phosphate derivatives and a Cu smelter plant are the most important industrial activities in Punta del Sebo estate. The Cu production process is said to be responsible of significant emissions of SO_2, As, Sb, Pb, Zn and Sn (González-Castanedo et al., 2014).

Very close to Nuevo Puerto facilities (SW) tons of raw materials in bulk are handled by dockers, including the transport and handling of, among others, coal, ore sulfide concentrates, clinker and coke, generating PM emissions into the atmosphere. The cargo is normally unloaded from ships to a hopper with a crane and then from hoppers to trucks to be transported. This material is also moved and piled by wheel dozers. Therefore, the high probability of resuspension when they are handled can entail dust emissions affecting to nearby zones.

It is also important to note that all the industrial activities mentioned above are beside and even inside the natural site Marismas del Odiel (Fig. 1), a high value ecosystem. Thus, a sustainable development of the activities is needed in order to improve the environmental quality of this area.

Most of the prior studies on air quality in Huelva are based on the industrial impact on urban air quality in order to know the effects over its population. However, the nearby populated area to the industries has hardly been considered. La Rabida is a small town situated at the SE of Huelva, crossing the Tinto River (Fig. 1), between the industrial areas Punta del Sebo and Nuevo Puerto, and it can be considered as an urban area with industrial influence affected by two types of emissions: channelized and fugitive.

2.2. Sampling

High volume PM10 sampling for chemical analysis was carried out at two monitoring stations:

- La Rabida: urban monitoring station with industrial influence. It is situated on the SE part of the estuary of Huelva (Fig. 1), halfway between the two industrial estates.
- Campus: urban background monitoring station located in the El Carmen University campus within the city of Huelva (Fig. 1).

At both monitoring sites sampling was performed using quartz fiber filters (MUNKTELL) and MCV high volume captors (30 m^3 h^{-1}) following the normalized method UNE-EN 12341, 2015. One daily sample (24 h) was collected every four-six days during the study period (2015–2017). The total number of samples collected was 197 at La Rabida and 183 at Campus monitoring stations. Before sampling, filters were heated 200 °C for 4 h and conditioned for 48 h at 20 °C and 50% of relative humidity. Then they were weighed by standard procedures in order to calculate the gravimetric PM10 concentration.

Furthermore, a 21-year record (January 1996–December 2017) of PM10 and gaseous pollutants levels was carried out at Campus and La Rabida monitoring stations. Both stations are equipped with automatic instrumentation to monitor hourly data of NO_2 (chemiluminescence), SO_2 (UV fluorescence), O_3 (UV photometry) and PM10 (beta attenuation) following the reference methods of the European directive on air quality (EU, 2008). Meteorological measurements as wind direction, wind speed, temperatures and relative humidity were obtained from the same station.

European directive (EU, 2008) establishes specific techniques and methodologies to determine particulate matter levels. However, it is possible to use another kind of equipment if their measures can be corrected by comparing to the European reference method. Thus, PM10 data measured by automatic equipment were corrected with those obtained from high volume captors MCV. The inter-comparison factor obtained (Table S1 on Supplementary Data) was approximately 1, so values from automatic methods could be considered.

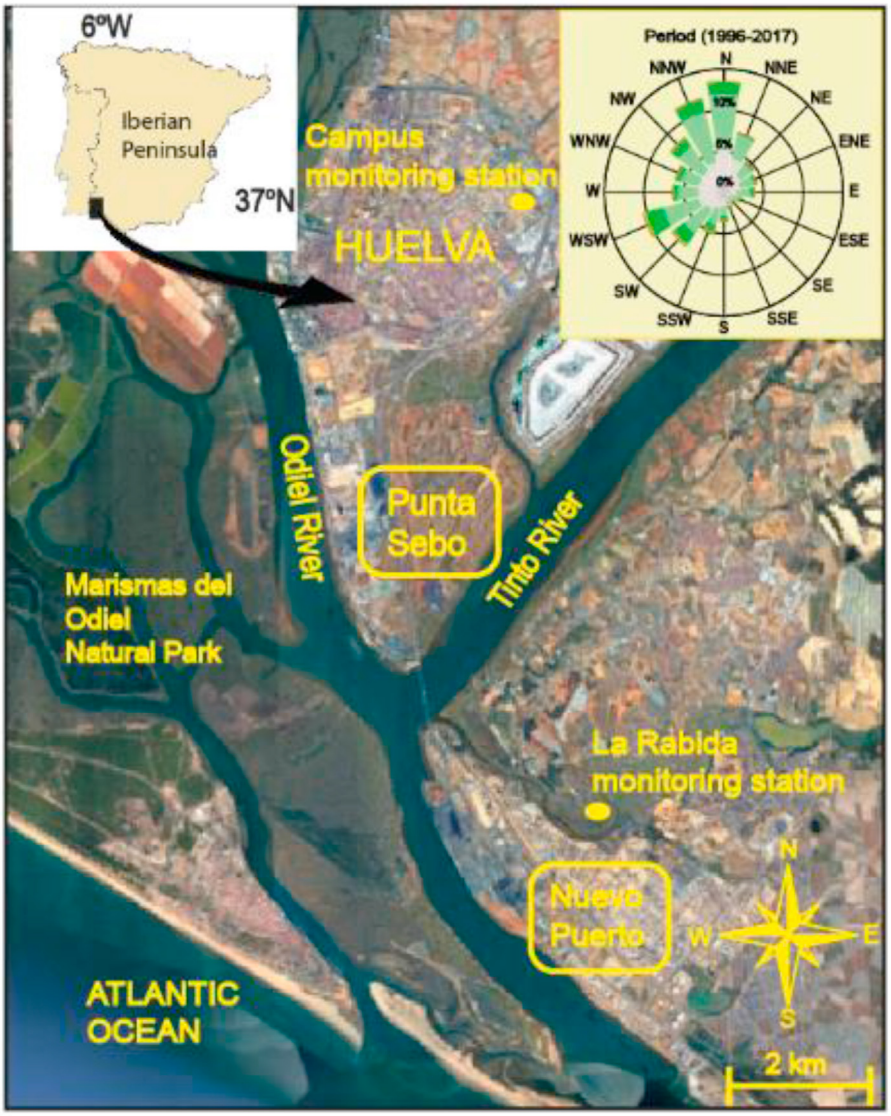

Fig. 1. Location map of sampling sites (Campus and La Rabida monitoring stations). Squares indicate industrial estates.

2.3. Sample treatment and chemical analysis

Prior to chemical analysis, sampled filters were placed in a desiccator for 24 h at 20 °C and 50% relative humidity, following standard procedures (UNE, 2015). They were then weighed in a Sartorius LA 130 S–F balance. Once PM10 levels were obtained by standard gravimetric methods, filters were subjected to several analytical treatments following the method proposed by Querol et al. (2001). A half fraction of each filter was acid digested (2.5 mL HNO_3: 5 mL HF: 2.5 mL $HClO_4$) for the analysis of major and trace elements by ICP-OES (Jobin Yvon model ULTIMA2) and ICP-MS (Agilent model 7900), respectively. For quality control, analysis of the NIST-1663 b (fly ash, Reference Standard Material) was carried out during every analytical run of both ICP techniques. External calibration was performed in ICP-MS by using cocktail solutions (1, 10, 50, 100 and 250 ppb as well as a HNO_3 5% blank). With the aim of minimizing the possible fluctuations of the plasma, ^{103}Rh was used as internal standard. The external calibration for ICP-OES was performed using elemental standards solutions (0.05–100 ppm and a HNO_3 5% blank). Accuracy and precision were in the range of 5–10% for the elements studied.

Another quarter of the filter was leached with Milli-Q grade deionized water in order to extract water soluble ions (SO_4^{2-}, NO_3^-, Cl^- and NH_4^+) for the subsequent analysis by ion chromatography (Methrom 883 Basic IC Plus) (Querol et al., 2002). The quality control of the results for soluble water ions were determined by solution cocktails for low and high range of cations (1–10 ppm) and anions (0.05–2.5 and 0.5–50 ppm). The accuracy and detection limit for IC was 10% and 0.4 μg m^{-3}. Finally, a portion of 1.5 cm^2 of each filter was used for the analysis of organic carbon and elemental carbon (OC and EC) using a Sunset Laboratory OC-EC Analyzer and following the EUSAAR-2 protocol (Cavalli et al., 2010). In this technique, an external sucrose aqueous solution was used in order to ensure the consistent operation of the instrument and the quality of the measurements.

SiO_2 and CO_3^{2-} concentrations were indirectly calculated by stoichiometry from the contents of Al, Ca and Mg, on the basis of experimental equation established by Querol et al. (2001): ($3Al_2O_3 = SiO_2$; $1.5Ca + 2.5\ Mg = CO_3^{2-}$). $SO_4^{2-}{}_{\text{non-sea salt}}$ was obtained by subtracting the $SO_4^{2-}{}_{\text{sea salt}}$ (indirectly calculated by

stoichiometry from the soluble Na levels) from $SO_4^{2-}{}_{total}$.

For As speciation, circular fractions (1.2 cm^2) of each PM10 sample were cut using a hollow and sharp-edged steel cylinder (diameter 1.24 cm). These circular portions were extracted by using a 100 mmol L^{-1} of $NH_2OH{\cdot}HCl$ solution as the extractant with the aid of microwave radiation (domestic microwave Samsung TDS, operated at 100 W) for 4 min. This procedure has been previously carried out for As speciation of TSP, PM10 and PM2.5 samples (Sánchez-Rodas et al., 2012). A QA/QC study of the extraction procedure of arsenic in atmospheric particulate matter has been described in Oliveira et al. (2005). The determination of individual inorganic As species (As(III) and As(V)) was achieved by coupling High Performance Liquid Chromatography, Hydride Generation and Atomic fluorescence Spectrometry (HPLC-HG-AFS). The detection limits obtained were of 0.1 ng m^{-3} for As(III) and 0.4 ng m^{-3} for As(V).

2.4. Statistical treatment and PMF

A temporal trend analysis was performed in the pollutant concentrations during the study period by using the Theil-Sen statistical estimator (Theil, 1950; Sen, 1968), available in the Openair package for R (Carslaw and Ropkins, 2012; Carslaw, 2015). The Theil-Sen function allows the calculation of the regression parameters of the data trend, including slope, uncertainty in the slope and the p value (significance of the trend). Monthly PM10 and gaseous pollutants mean values were calculated for hourly resolution data. The symbols shown next to the trend estimate relate to how statistically significant the trend estimate is: $\rho < 0.001$ = ***, $\rho < 0.01$ = **, $\rho < 0.05$ = *, $\rho < 0.1$ = +; no symbol stands for no significant trend.

The chemical speciation data of the collected daily PM10 samples were used within the Positive Matrix Factorization model (PMF v5.0 EPA) for source identification and apportionment. The PMF model is a factor analytical tool to calculate the contributions and chemical profiles of the sources affecting the receptor site using ambient species concentrations. It was developed by Paatero and Tapper (1994) and it is explained in detail by Paatero (1997). PMF is based on the following mathematic algorithm:

$$\chi_{ij} = \sum_{k-1}^{p} g_{ik} * f_{kj} + e_{ij}$$

The data set can be expressed as a matrix x of i by j dimensions, where i is the number of samples and j is the chemical elements measured. Additionally, p is the number of independent factors, g_{ik} is the amount of mass contributed by each factor for each individual sample, f_{kj} represents the species profiles of each factor, and e_{ij} is the residue for each sample by element.

PMF is a weighted least-squares method so that individual estimates of the uncertainty in each data value are needed in order to be included in the input matrix. There are several sources of error contributing to the measurements uncertainty, but the associated with the analytical procedure is probably one of the most important. The uncertainties were calculated following the methodology proposed by Amato et al. (2009).

Elements were classified using the signal-to-noise S/Nj ratio defined by Paatero and Hopke (2003). Those elements with S/N < 2 were generally defined as weak variables. Since S/N ratio is very sensitive to sporadic values much higher than the level of noise, the percentage of data above detection limit was used as complementary criterion.

3. Results and discussion

3.1. Annual time series of gaseous pollutants and PM_{10} levels

Data availability of PM10, NO, NO_2, NO_X, SO_2 and O_3 between February 1996 and December 2017 at La Rabida and Campus monitoring stations enabled us to calculate mean annual levels of these pollutants during this period (Table S2, Fig. 2). In order to evaluate time trends, mean concentrations were plotted and analyzed for statistical significant trends. Hourly, daily, weekly and seasonal cycles were also calculated (Fig. S2).

3.1.1. NO_2

NO_2 levels at both monitoring sites diminished during the study period, with a decrease rate of −0.53 and −0.93 μg $m^{-3}{\cdot}year^{-1}$ at Campus and La Rabida stations, respectively (Fig. 2). The concentrations of NO_2 showed a noticeable reduction since 2009 with low values until the end of the period. Even in the early years when mean levels were maximum (31 μg m^{-3} La Rabida in 1998), the European Union NO_2 annual standard (40 μg m^{-3}, EU, 2008) was not exceeded. NO_2 has strong traffic and industrial origin, and hence the Spanish economic crisis (around 2008) caused a diminution of these sources. At the end of the period, NO_2 values remained constant possibly due to the economy recovery from the crisis and the development of emission reduction technology.

Mean hourly levels of NO2 at the two monitoring stations showed two maxima during the working days at rush hours early in the morning and in the evening. These peaks point to vehicle exhaust and industrial emissions as the main responsible of NO_2 concentrations. Regarding seasonal patterns (Fig. S2), NO_2 levels were higher in winter, which is typical from pollutants related to traffic. However, high concentrations during the summer were also observed. In this way, a detailed study of the pollutant was carried out over the year and it suggested an industrial source of NO_2. Two predominant wind directions were identified at La Rabida in the summer months: NW, where Punta del Sebo industrial estate is located and SE, proceeding from Nuevo Puerto industrial estate. In the same way, the high NO_2 concentrations at Campus in May come from the SW direction, pointing to industrial emissions. According to the polar plot (Fig. S3 on Supplementary Data), NO_2 concentrations in the evenings may be due to the regional traffic pollution, whereas in the morning (8:00–9:00) NO_2 levels point to both traffic and industrial sources.

3.1.2. SO_2

SO_2 concentrations showed a very similar pattern in both monitoring stations. Levels decreased considerably in 2001 at La Rabida (7 μg m^{-3}), increasing afterwards until 2007 (13 μg m^{-3}). After that, concentrations diminished until a minimum value of 5 μg m^{-3} in 2015. At Campus monitoring station, SO_2 concentrations also showed a smooth increase until 2009 (10 μg m^{-3}) with a subsequent decrease that finished in 2015 (5 μg m^{-3}). Even though there is not an annual SO_2 limit stablished, the European normative recommends not exceeding more than 24 times per year 350 SO_2 $\mu g{\cdot}m^{-3}{\cdot}h^{-1}$. This target value is rarely exceeded, however sporadic hourly SO_2 peaks (>20 μg m^{-3} h^{-1}) have been measured during the study period. The number of days with SO_2 impacts has diminished throughout the years (Fig. S5), as well as the concentration corresponding to these peaks, due to the implementation of emission abatement technologies in the Cu smelter during the study period (Sánchez de la Campa et al., 2018).

Regarding the number of days per month with SO_2 impacts (Fig. S5), there is a seasonal pattern at Campus with highest number of impact days in the warmer months. At La Rabida station, a high

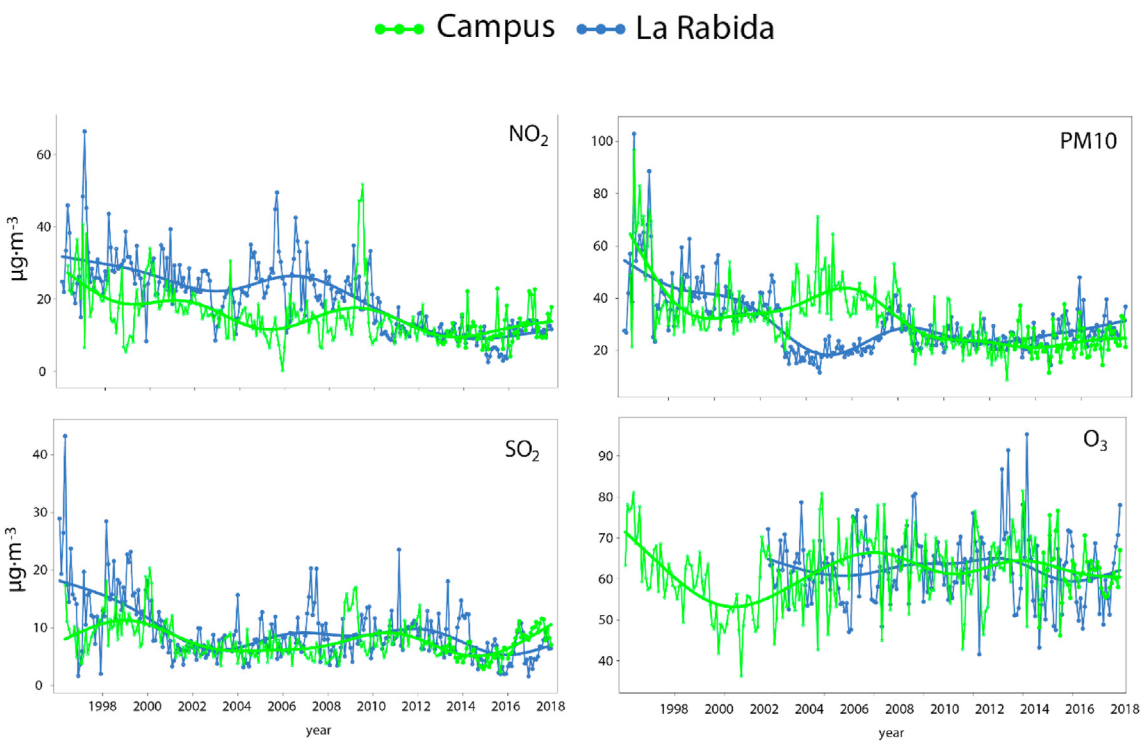

Fig. 2. Annual variation of gaseous pollutants and PM10 at Campus (2008–2017) and La Rabida (1996–2017) monitoring stations.

number of SO_2 impact days can also be observed in January and February as a consequence of its closeness to the industrial estates. The combined effect of the pollution abatement strategies and the economy recession caused the reduction of this anthropogenic pollutant for the end of the period (-0.25 µg m^{-3}·$year^{-1}$).

Considering SO_2 concentrations at La Rabida, mean hourly levels were higher between 0-5 h and 12–15 h as a consequence of the prevailing wind from the NW direction. On the other hand, high values of SO_2 concentrations are found at Campus monitoring station between 14 and 18 h, when the SW component dominates the wind direction (Fernández-Camacho et al., 2010). Although there is not a clear seasonal pattern, SO_2 concentrations increased in March, July, August and December (Fig. S2). It has been demonstrated the industrial provenance of SO_2 in Huelva and its relationship with toxic elements (Fernández-Camacho et al., 2010; Sánchez de la Campa et al., 2018). The main SO_2 emission sources in La Rabida are derived from petrochemical activities, a Cu smelter and the production of TiO_2 pigments, being their contribution in 2016 56, 40 and 4%, respectively (Spanish Register of Emissions and Pollutant Sources; PRTR, 2016). This idea can be supported considering the SO_2 provenance coming mostly from NW direction (Cu smelter) but a secondary source can be observed in the SE (oil refinery and TiO_2 production).

3.1.3. O_3

O_3 concentrations remained constant from 2003 to 2017 at both monitoring stations (0.33 and 0.12 µg m^{-3}·$year^{-1}$ at Campus and La Rabida, respectively).

O_3 levels reached maximum values everyday between 15 and 20 h (Fig. S2) at both monitoring stations, coinciding with the diurnal time when sun light intensity is higher and when sea breeze air transport prevails. In the same way, O_3 showed a seasonal pattern characterized with maximum concentrations during the warmer months.

3.1.4. PM10

In the case of PM10, a pronounced decrease can be seen at La Rabida in 2003 (Fig. 2) followed by higher concentrations until 2007, decreasing afterwards, at both monitoring stations at a rate of -1.07 and -0.80 µg m^{-3}·$year^{-1}$ at Campus and La Rabida, respectively. The European annual target value of 40 µg m^{-3} (EU, 2008) was not exceeded during the latest years.

PM10 concentrations experiment a noticeable raise during the working days between 17 and 20 h. According to the seasonal evolution, maximum values of PM10 occur in the warmer months and March, when Sahara dust events and dry periods are more frequent (Viana et al., 2002). However, regarding the summer months at La Rabida, when the typical SW breeze occurs in the afternoon, an important PM10 source were found coming from this direction. This source is attributable to the regional anthropogenic emissions caused by handling loose materials by the dockers. Moreover, the lack of rainfalls during the summer enhances these fugitive emissions. At Campus station high PM10 concentrations are observed in the evening coming from the N direction where local roads and a highway are located and the resuspension is more likely to occur.

It is also important to emphasize the relatively low PM10 annual concentrations obtained at La Rabida during the latest years of the period (32 µg m^{-3}, 27 µg m^{-3}, and 30 µg m^{-3} in 2015, 2016 and 2017 respectively). Therefore, the EU air quality annual standard (EU, 2008) of 40 µg PM10·m^{-3} was not exceeded during these years. Besides that, the number of exceedances of the daily European limit value 50 µg PM10·m^{-3} recorded at the end of the period (2015–2017) were 53 days, 43 of which were attributable to North African dust outbreak (NAF) coming from Saharan air masses. In this way, the maximum of the 35 days of exceedances imposed by the European normative was not exceeded in any of the years 2015, 2016 and 2017 (27, 8 and 18 days of exceedances accordingly). Most of the NAF daily exceedances recorded in this latest period were observed mainly in February, March and in the summer. However,

when the daily exceedances were due to anthropogenic sources, high concentrations of PM10 were showed in March, April, August, September and December, with a non-defined pattern.

3.2. Chemical composition of PM10

Mean levels of PM10, major components and trace elements and its annual statistical trend at both monitoring stations (Campus and La Rabida) during the period 2015–2017 are showed in Table S2.

The mean PM10 inter-annual concentrations, gravimetrically measured from Campus and La Rabida stations for the period 2015–2017, were 29 and 32 μg m^{-3} respectively, in agreement with the PM10 range reported by Querol et al. (2012) for urban backgrounds with industrial influence (28–47 μg m^{-3}). Therefore, the annual 40 μg PM10·m^{-3} limit fixed by the European Directive (EU, 2008) was not exceeded at the two considered monitoring stations.

Regarding PM10 components, high concentrations of mineral dust have been found at the two monitoring stations (8.92–9.51 μg m^{-3}), within the range described for urban-industrial backgrounds (6–13 μg m^{-3}, Querol et al., 2008). Moreover, crustal components in the two monitoring stations have increased their concentrations over time. Considering the time plots of these pollutants, sporadic peak concentrations were found during the months February–March every year, being correlated with the Saharan dust outbreak events (Pey et al., 2013).

The contribution of secondary inorganic compounds (sum of NO_3^-, NH_4^+, SO_4^{2-}) does not reach annual average concentrations higher than 6 μg m^{-3}. These values are lower than those found in earlier works performed at urban monitoring stations in Huelva (Fernández-Camacho et al., 2010). NO_3^- concentrations (1.95–2.09 μg m^{-3}) are consistent with the concentrations values previously observed in Huelva (Querol et al., 2012). Non-sea salt SO_4^{2-} does not reach levels higher than 4 μg m^{-3}. Time series of anthropogenic SO_4^{2-} exhibited a seasonal evolution with levels slightly higher in summer-autumn (Fig. S6), resulting from the increased oxidation of SO_2 to SO_4^{2-} that occurs in this warm period (Harrison et al., 1996; Pio et al., 1998). A converse seasonal pattern is shown by NO_3^- as a consequence of the low thermal stability of NH_4NO_3 in summer, resulting in the formation of the gaseous nitric acid and ammonia (Adams et al., 1999). In contrast to SO_4^{2-} and NO_3^- concentrations, NH_4^+ levels presented a bimodal seasonal variation over the 3 years of the study: values normally increase during the summer time but, on the other hand, winter peak concentrations were also observed in the time variation plot (Fig. S6). NH_4^+ measured in the cooler months is due to the formation of NH_4NO_3, whereas in the summer period $(NH_4)_2SO_4$ is the dominant specie, as it has been explained before (Cusack et al., 2012).

Annual concentrations of carbonaceous particles (OC + EC: organic and elemental carbon), ranged from 3.94 to 4.06 μg m^{-3} as expected for this urban-industrial environment (Querol et al., 2012). OC + EC concentrations were higher at Campus station since these PM10 components come mainly from vehicle exhaust and industrial combustion.

The mean contribution (2.72 and 2.91 μg m^{-3} at Campus and La Rabida monitoring stations, respectively) of sea salt aerosols (Na^+, Cl^- and sea salt SO_4^{2-}) was within the typical range for Atlantic coastal sites in the Iberian Peninsula (Querol et al., 2008). Maximum concentrations of Na^+ were obtained in summer as a consequence of the stronger influence of see breezes, whereas Cl^- levels were lower during the summer months due to its volatilization as HCl derived from the formation of $NaNO_3$ by interaction of the gaseous HNO_3 and sea salt NaCl. It should be noted the partial anthropogenic origin of Cl^-, which can be observed in the Cl^- excess presented in some peak events.

In reference to the trace elements, As was found to be the main geochemical anomaly in PM10. Annual mean concentrations at La Rabida (7.95, 6.18 and 6.76 μg m^{-3} in 2015, 2016 and 2017, respectively) were above the target value recommended by the EU (6 ng As·m^{-3}, EU, 2004). On the other hand, mean As concentrations measured in Campus were lower for the whole period (2.96, 3.05 and 2.46 μg m^{-3} in 2015, 2016 and 2017, respectively). Concentrations values were consistent with those reported by Sánchez de la Campa et al. (2018) in urban stations in Huelva in recent years (2014–2015). Nevertheless, it is important to note the decrease of the As concentrations in 2017 with regard to 2015. La Rabida monitoring station is very close to the industrial area where the Cu smelter is located, and high As concentrations have been previously described as a result of its emissions (González-Castanedo et al., 2014).

Cu and Zn concentrations at Campus are similar to the values obtained by Querol et al. (2008) at urban monitoring sites of Spain. However, higher concentration are observed at La Rabida as a consequence of polymetallic sulfides handling near the station. Bi (0.93 ng m^{-3}) and Se (0.46 ng m^{-3}) at La Rabida have also characteristic values for a station close to a Cu smelter. Levels of V (6.13 ng m^{-3}) and Ti (71.4 ng m^{-3}) were especially high at La Rabida probably due to the emissions from a petrochemical plant and a TiO_2 production facility developed in Nuevo Puerto estate (Alastuey et al., 2006). Concerning other elements with limit target values in the EU air quality standards such as Pb, Ni and Cd, none of them exceeded air quality thresholds (500 ng Pb·m^{-3}, EU, 2008; 20 ng Ni·m^{-3} and 5 ng Cd·m^{-3}; EU, 2004) in none of the monitoring stations. Although As, Cu and Pb did not show a clear seasonal variation, they presented random maximum peaks which probably come from the close Cu smelter or from the industrial activity.

It is important to emphasize the similar concentrations of mayor components of PM10 at both monitoring stations with the exception of Fe that may originate from the mineral fugitive emissions occurred near La Rabida station. Concerning trace elements, the high values of As, Cu, Zn and Pb at La Rabida showed a stronger industrial influence in this monitoring station.

3.3. Source apportionment analysis

A PMF analysis was performed for both monitoring stations in order to identify the natural and anthropogenic sources contributing to PM10 over the period 2015–2017. Fig. S7 shows the chemical profiles and the species percentage for each source. 5 sources were identified at Campus monitoring station: crustal 1, crustal 2, aged sea salt, Cu smelter, and traffic-biomass burning. In the case of La Rabida station, 6 sources were found: traffic, crustal, aged sea salt, regional, Cu smelter and sulfides (Fig. 3).

The crustal source is characterized by the typical silicate components as Al_2O_3, Fe, Ca, Rb, Ti, Mn and Sr. The long-range transport dust and the local resuspension are the main contributing factors of this source. Similar crustal contribution were reached at Campus monitoring site (Crustal 1: 5.3 μg m^{-3}, 19%) and La Rabida (5.0 μg m^{-3}, 16%), affected by urban and industrial resuspension, respectively. A second crustal source (Crustal 2: 3.9 μg m^{-3}, 14%) was found at Campus showing high concentrations of Y and Th. Apart from that, La Rabida is also influenced by the handling of bulk material.

The traffic source represents a higher PM10 contribution at Campus (10.6 μg m^{-3}, 39%) than at La Rabida (8.8 μg m^{-3}, 29%). It is characterized by high loads of NO_3^-, NH_4^+, EC and OC, deriving from vehicle exhausts emissions. This factor is also made up by high concentrations of Ca, K, Ti, Cr, Sn, and Sb; attributed to non-exhaust vehicle emissions (Amato et al., 2014), mostly from the brake and

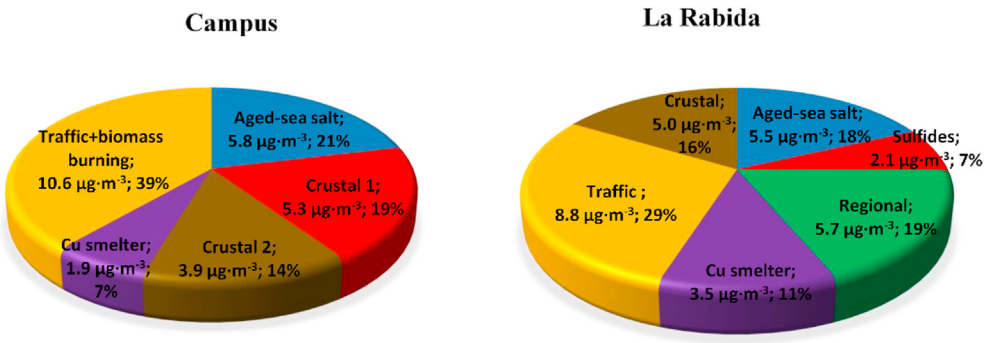

Fig. 3. Percentage source apportionment of PM10 mass.

tyre wear as well as the road dust resuspension. Regarding traffic profile in Campus monitoring station, the presence of PO_4^{3-} points to emissions from biomass burning. Levels of these compounds were higher in the winter months, since the planetary boundary layer is reduced and pollutants are concentrated in the atmosphere.

A regional source was identified at La Rabida (5.7 μg m^{-3}, 19%) with SO_4^{2-}, NO_3^- and NH_4^+ as typical components. These components are associated to PM usually derived from emissions of petrochemical activities and the production of phosphates derivatives (Ni, V, Co, Sn, Pb, Sb, Cr, Mn and Fe). This relationship has been previously reported by other authors (Querol et al., 2002; Alastuey et al., 2006). Levels of this source were higher in summer as a consequence of the coupling of refinery emissions to the air masses proceeding from North Africa with predominant SW wind direction (Pandolfi et al., 2014).

An aged sea salt source was identified at both monitoring stations. The typical sea salt components (Na, Cl and Mg) showed similar contribution at Campus (5.8 μg m^{-3} 21%) and La Rabida (5.5 μg m^{-3}, 18%). This component was also characterized by the presence of Sr as a result of the dust resuspension.

In relation to the Cu smelter, a single source was isolated at the two monitoring stations considered in this work. These emissions arise from Cu smelting operations that take place in the Punta del Sebo industrial estate. They include high concentrations of As, Bi, Pb, Sb, Sn, Se, Cd, Cu and Zn; and accounted for 1.9 μg m^{-3} (7%) and 3.5 μg m^{-3} (11%) at Campus and La Rabida, respectively. Concerning the time evolution of this component, sporadic peaks are related to certain meteorological conditions which cause the impact of emissions from the Cu smelter. This source has been broadly described in early works in the city of Huelva (e.g. Fernández-Camacho et al., 2010). Furthermore, a sulfide-mineral source was also identified at La Rabida with a contribution of 2.1 μg m^{-3} (7%). The high loads of Cu, Fe, Zn, Ni, Cd, Co, As, Sb and Bi suggest a geochemical profile typical from sulfide mineral concentrates. Polymetallic sulfide mineral are specifically unloaded by the dockers in the port and fugitive dust could be emitted, affecting directly to the nearby area.

3.4. Arsenic speciation in PM10

The European Air Quality normative (EU, 2004) only considers the total content of As in PM10, with a target annual value of 6 ng m^{-3} of As in PM10. However, the degree of toxicity of As varies depending on its oxidation state or molecular structures it may be present. In this way, inorganic species such as arsenite and arsenate (As(III) and As(V)), are more harmful than methylated species. Of the two inorganic species, As(III) is more toxic than As(V) because of their interaction with sulfhydryl groups of proteins and enzymes inhibiting their function (Francesconi and Kuehnelt, 2004). The main anthropogenic emissions of As to air in the study area come from the smelting of metals and the combustion of fuels, gas and carbon. However, recent studies have also evaluated the presence and release of As from dust material handled by the dockers like coal, clinker, or ore sulfide mineral (Moreno et al., 2009). Moreover, As-bearing sulfide is the most common form of inorganic As found in coal, and it is also associate with Cu, Pb and Zn sulfides (Liu et al., 2007).

In this sense, it was possible to determine different types of As sources (channeled and fugitive) by means of As speciation analysis, combining the As extraction of the sampled filters, wind direction and SO_2 peaking days. A total of 33 PM10 samples with high As concentrations were selected during the period 2015–2016 at the two monitoring stations considered in this study. Most of the samples correspond to synchronic sampling of PM10, in order to compare results of the same days.

The ranges of As concentrations of the selected PM10 samples with high levels of this metalloid are shown in Table 1 at Campus and La Rabida monitoring stations. As(III) and As(V) concentrations determined by HPLC-AF-HG, as well as the extraction percentage obtained from PM10 samples and the dominant wind direction are also reported in Table 1. These parameters are specified for both monitoring stations depending on the major As source. There are two main As emission sources near the monitoring stations, a channelized one corresponds to a Cu smelter industry located in the Punta del Sebo industrial estate, and fugitive emissions attributable to the bulk material handled by the dockers (mostly ore sulfide concentrate). The distinction between both sources can be related to the efficiency of As extraction. In the case of the Cu smelter, As is quantitatively extracted (>80%) from PM10 probably because it is occurring in high temperature fly ash or slag particles resulting from oxidative metallurgy. On the other hand, in the bulk material accumulated in the dock, As is an impurity of the polymetallic sulfides, from which As is poorly extracted. Regarding to these two As emission sources, three different scenarios can be considered concerning the possible impact on the monitoring sites:

(a) Impact from metallurgy emissions: The As extraction efficiency is very high, (80–100%) (Table 1) and it is usually associated with SO_2 plumes originated from the Cu smelter emissions. This situation normally occurs at La Rabida when wind direction is dominated the NW component. However, at Campus monitoring site the SW component dominates the wind direction when the Cu smelter impact occurs.
(b) Impact from bulk polymetallic sulfides: This scenario includes the impact of the resuspension of sulfide mineral concentrates handled by dockers and the resuspension of sulfide of polluted soils around the city of Huelva (Torres et al., 2017). The As extraction efficiency is low (<20%,

Table 1
Classification of the different scenarios of As impacts in Campus and La Rabida monitoring stations in the period 2015–2016 according to arsenic sources (Cu smelter and sulfides concentrate). N indicates the number of samples and WD the wind direction.

PM10 Fraction	Campus			La Rabida		
	Cu smelter (N = 6)	Sulfides (N = 1)	Mixed (N = 4)	Cu smelter (N = 5)	Sulfides (N = 3)	Mixed (N = 6)
$ng \cdot m^{-3}$						
As(III)	0.6–0.0	0.0	0.1–0.3	0.2–0.0	0.3–0.7	0.2–0.7
As(V)	2.6–13.7	1.6	0.7–5.7	5.6–22.3	0.2–8.0	3.1–9.6
Species sum	2.7–14.0	1.6	3.3–10	5.8–22.3	0.9–8.3	3.3–10
Total As ICP-MS	3–15	16	5–21	6–24	25–45	5–21
% extraction	83–96	4–18	37–75	94–100	4–18	37–75
WD	N-NNW-NW	WSW-SW	N-NNW; WSW-SW	N-NNW-NW	WSW-SW	N-NNW; WSW-SW

Table 1) and the dominating wind components at La Rabida are SW or WSW with pointing to a sulfide origin source. Furthermore, As concentrations resulting from these fugitive emissions are much higher than those resulting from the metallurgy emissions.

(c) *Mixed impact.* The third scenario is an intermediate situation which occurs with a mix of the wind directions (primarily NW and SW components) along the day and causes the association of the two As sources at La Rabida monitoring site. This situation is the most frequent and is characterized by moderate extraction yields (30–70%) of As from PM10.

It is clear from the results that the most important As source comes from the Cu smelter emissions as it has been described in prior studies (Fernández-Camacho et al., 2010; González-Castanedo et al., 2014). However, there is a fugitive As source related to the handling by dockers of polymetallic sulfides which gives rise to episodic high As concentrations in PM10. In this sense, this methodology allows us to identify two different As origin (metallurgy and bulk polymetallic sulfides), which has not been taken into account previously in the same monitoring station.

The low percentage of As extraction of sulfide mineral compared with Cu smelter emission particles indicates low biodisponibility, and in consequence a small degree of hazardous for the environment. In consequence, the importance of the As origin relies on the requirement of investigating new strategies in order to reduce the emission of As that can affect to nearby areas.

4. Conclusions

A general decreasing trends were observed for the concentrations of gaseous pollutants and PM10 in the industrialized area of Huelva (SW Spain) in the period 1996–2017. This diminution is more evident since 2008 due to the economic recession and the enforcement of air quality European Directives. From a detailed analysis of the pollutants, it was inferred a strong industrial contribution of SO_2, whereas traffic emissions contributed to NO_2 levels. The high resuspension proceeding from the bulk sulfide material handled by the dockers enhanced PM10 concentrations, especially crustal components at La Rabida monitoring station.

Arsenic was found to be the main geochemical anomaly in PM10. Factorial analysis of the chemical composition of PM10 and As speciation analysis allowed to identify two As emission sources. One of them corresponds to Cu smelter emissions already described in the study area in prior studies. However, the second one is due to emissions that take place when bulk polymetallic sulfides are handled by the dockers. The low biodisponibility of As in the sulfide mineral implies a low hazardous impact for the air quality and human health. The results obtained in this study allowed us to identify for the first time two different sources contributing to the high As concentrations in the same place of a complex industrial area.

Sample CRediT author statement

María Millán Martínez: Investigation, Writing – original draft. Daniel Sánchez-Rodas: Reviewing, Methodology. Ana M. Sánchez de la Campa: Reviewing, Methodology. Andrés Alastuey: Methodology. Xavier Querol: Reviewing, Methodology. Jesús D. de la Rosa: Funding acquisition, Reviewing.

Declaration of competing interest

The authors declare that they have no known competing financial interests or personal relationships that could have appeared to influence the work reported in this paper.

Acknowledgments

We would like to acknowledge the project of Ministry of Science, Innovation and Universities of Spain (Project RTI2018-095937-B-I00) and Environmental Agency of Andalusia for financial and technical support.

Appendix A. Supplementary data

Supplementary data to this article can be found online at https://doi.org/10.1016/j.envpol.2020.116268.

References

Adams, P.J., Seinfeld, J.H., Koch, D.M., 1999. Global concentrations of tropospheric sulphate, nitrate, and ammonium simulated in a general circulation model. J. Geophys. Res. 104, 13791–13823. https://doi.org/10.1029/1999JD900083.

AEMET (Spanish State Meteorological Agency), 2019. last accessed 2020. https://opendata.aemet.es/centrodedescargas/productosAEMET.

Alastuey, A., Querol, X., Plana, F., Viana, M., Ruiz, C.R., de la Campa, Sánchez, de la Rosa, J., Mantilla, E., García dos Santos, S., 2006. Identification and chemical characterization of industrial particulate matter sources in southwest Spain. J. Air Waste Manag. Assoc. 56, 99–1006. https://doi.org/10.1080/10473289.2006.10464502.

Amato, F., Pandolfi, M., Escrig, A., Querol, X., Alastuey, A., Pey, J., Perez, N., Hopke, P.K., 2009. Quantifying road dust resuspension in urban environment by multilinear engine: a comparison with PMF2. Atmos. Environ. 43, 2770–2780. https://doi.org/10.1016/j.atmosenv.2009.02.039.

Amato, F., Alastuey, A., de la Rosa, J., Gonzalez-Castanedo, Y., Sánchez de la Campa, A.M., Pandolfi, M., Lozano, A., Contreras González, J., Querol, X., 2014. Trends of road dust emissions contributions on ambient air particulate levels at rural, urban and industrial sites in southern Spain. Atmos. Chem. Phys. https://doi.org/10.5194/acp-14-3533-2014.

Belis, C.A., Cancelinha, J., Duane, M., Forcina, V., Pedroni, V., Passarella, R., Tanet, G., Douglas, K., Piazzalunga, A., Bolzacchini, E., Sangiorgi, G., Perrone, M.G., Ferrero, L., Fermo, P., Larsen, B.R., 2011. Sources for PM air pollution in the Po Plain, Italy: I. Critical comparison of methods for estimating biomass burning contributions to benzo(a)pyrene. Atmos. Environ. 45, 7266–7275. https://doi.org/10.1016/j.atmosenv.2011.08.061.

Calvo, A.I., Alves, C., Castro, A., Pont, V., Vicente, A.M., Fraile, R., 2013. Research on aerosol sources and chemical composition: past, current and emerging issues. Atmos. Res. 120–121, 1–28. https://doi.org/10.1016/j.atmosres.2012.09.021.

Carslaw, D.C., 2015. The Openair manual — open-source tools for analysing air pollution data. In: Manual for Version 1.5-9, King's College London.
Carslaw, D.C., Ropkins, K., 2012. OpenAir: an R package for air quality data analysis. Environ. Model Softw. 27 (28), 52–61. https://doi.org/10.1016/j.envsoft.2011.09.008.
Cavalli, F., Viana, M., Yttri, K.E., Genberg, J., Putaud, J.-P., 2010. Toward a standardized thermal–optical protocol for measuring atmospheric organic and elemental carbon: the EUSAAR protocol. Atmos. Meas. Technol. 3, 79–89. https://doi.org/10.5194/amt-3-79-2010.
Chen, B., Stein, A.F., Castell, N., Gonzalez-Castanedo, Y., Sánchez de la Campa, A.M., de la Rosa, J.D., 2016. Modeling and evaluation of urban pollution events of atmospheric heavy metals from a large Cu-smelter. Sci. Total Environ. 539, 17–25. https://doi.org/10.1016/j.scitotenv.2015.08.117.
Cusack, M., Alastuey, A., Pérez, N., Pey, J., Querol, X., 2012. Trends of particulate matter (PM2.5) and chemical composition at a regional background site in the Western Mediterranean over the last nine years (2002–2010). Atmos. Chem. Phys. 12, 8341–8357. https://doi.org/10.5194/acp-12-8341-2012.
European Commission, 2004. Directive 2004/107/EC relating to arsenic, cadmium, mercury, nickel and polycyclic aromatic hydrocarbons in ambient air. last accessed July 2017. https://bit.ly/2PQHh7W.
European Commission, 2008. Directive 2008/50/CE on ambient air quality and cleaner air for Europe. Last Accesed July 2017. https://bit.ly/2R7Peu3.
Fernández-Camacho, R., de la Rosa, R., Sanchez de la Campa, A.M., González-Castañedo, Y., Alatuey, A., Querol, X., Rodríguez, S., 2010. Geochemical characterization of Cu-smelter emission plumes with impact in an urban area of SW Spain. Atmos. Res. 96, 590–601. https://doi.org/10.1016/j.atmosres.2010.01.008.
Fernández-Camacho, R., Rodríguez, S., de la Rosa, J.D., Sánchez de la Campa, A.M., Alastuey, A., Querol, X., González-Castanedo, Y., García-Orellana, I., Nava, S., 2012. Source apportionment of ultrafine particles in Huelva industrial city. Atmos. Environ. 61, 507–517. https://doi.org/10.1016/j.atmosenv.2012.08.003.
Francesconi, K.A., Kuehnelt, D., 2004. Determination of arsenic species: a critical review of methods and applications (2000–2003). Analyst 129 (5), 373–395. https://doi.org/10.1039/B401321M.
Gieré, R., Querol, X., 2010. Solid particulate matter in the atmosphere. Elements 6 (4), 215–222. https://doi.org/10.2113/gselements.6.4.215.
González-Castanedo, Y., Moreno, T., Fernández-Camacho, R., Sanchez de la Campa, A.M., Alastuey, A., 02Querol, X., Rosa, J., 2014. Size distribution and chemical composition of particulate matter stack emissions in and around a copper smelter. Atmos. Environ. 98, 271–282. https://doi.org/10.1016/j.atmosenv.2014.08.057.
Harrison, R., Smith, D., Luhana, L., 1996. Source apportionment of atmospheric polycyclic aromatic hydrocarbons collected from an urban location in Birmingham, UK. Environ. Sci. Technol. 30, 825–832. https://doi.org/10.1021/es950252d.
Hopke, P.K., 2016. A review of receptor modeling methods for source apportionment. J. Air Waste Manag. Assoc. 66, 237–259. https://doi.org/10.1080/10962247.2016.1140693.
Li, J., Chen, B., Sánchez de la Campa, A.M., Alastuey, A., Querol, X., de la Rosa, J.D., 2018. 2005-2014 trends of PM10 source contributions in an industrialized area of southern Spain. Environ. Pollut. 236, 570–579. https://doi.org/10.1016/j.envpol.2018.01.101.
Liu, G., Zheng, L., Zhang, Y., Qi, C., Chen, Y., Peng, Z., 2007. Distribution and mode of occurrence of as, Hg and Se and sulfur in coal seam 3 of the Shanxi formation, Yanzhou Coalfield, China. Int. J. Coal Geol. 71, 371–385. https://doi.org/10.1016/j.coal.2006.12.005.
Lee, P.K.H., Brook, J.R., Dabek-Zlotorzynska, E., Mabury, S.A., 2003. Identification of the major sources contributing to PM2.5 observed in Toronto. Environ. Sci. Technol. 37 (21), 4831–4840. https://doi.org/10.1021/es026473i.
Monteiro, A., Russo, M., Gama, C., Lopes, M., Borrego, C., 2018. How economic crisis influence air quality over Portugal (Lisbon and Porto)? Atmos. Pollut. Res. 9, 439–445. https://doi.org/10.1016/j.apr.2017.11.009.
Moreno, T., Querol, X., Alastuey, A., Viana, M., Salvador, P., Sánchez de la Campa, A.M., Artiñano, B., de la Rosa, J., Gibbons, W., 2006. Variations in atmospheric PM trace metal content in Spanish towns: illustrating the chemical complexity of the inorganic urban aerosol cocktail. Atmos. Environ. 40, 6791–6803. https://doi.org/10.1016/j.atmosenv.2006.05.074.
Moreno, N., Viana, M., Pandolfi, M., Alastuey, A., Querol, X., Chinchon, S., 2009. Determination of direct and fugitive PM emissions in a Mediterranean harbour by means of classic and novel tracer methods. J. Environ. Manag. 91, 133–141. https://doi.org/10.1016/j.jenvman.2009.07.009.
Oliveira, V., Gómez-Ariza, J.L., Sánchez-Rodas, D., 2005. Extraction procedures for chemical speciation of arsenic in atmospheric total suspended particles. Anal. Bioanal. Chem. 382, 335–340. https://doi.org/10.1007/s00216-005-3189-1.
Paatero, P., 1997. Least square formulation of robust non-negative factor analysis. Chemometr. Intell. Lab. Syst. 3, 23–35. https://doi.org/10.1016/S0169-7439(96)00044-5.
Paatero, P., Hopke, P.K., 2003. Discarding or down weighting high-noise variables in factor analytic models. Anal. Chim. Acta 490, 277–289. https://doi.org/10.1016/S0003-2670(02)01643-4.
Paatero, P., Tapper, U., 1994. Positive matrix factorization: a nonnegative factor model with optimal utilization of error estimates of data values. Environmetrics 5, 111–126. https://doi.org/10.1002/env.3170050203.
Pandolfi, M., Gonzalez-Castanedo, Y., Alastuey, A., Rosa, J.d.l., Mantilla, E., Campa, A.S.d.l., Querol, X., Pey, J., Amato, F., Moreno, T., 2011. Source apportionment of PM10 and PM2.5 at multiple sites in the strait of Gibraltar by PMF: impact of shipping emissions. Environ. Sci. Pollut. Res. 18, 260–269. https://doi.org/10.1007/s11356-010-0373-4.
Pandolfi, M., Tobias, A., Alastuey, A., Sunyer, J., Schwartz, J., Lorente, J., Pey, J., Querol, X., 2014. Effect of atmospheric mixing layer depth variations on urban air quality and daily mortality during Saharan dust outbreaks. Sci. Total Environ. 494–495, 283–289. https://doi.org/10.1016/j.scitotenv.2014.07.004.
Pey, J., Querol, X., Alastuey, A., Forastiere, F., Stafoggia, M., 2013. African dust outbreaks over the Mediterranean Basin during 2001–2011: PM10 concentrations, phenomenology and trends, and its relation with synoptic and mesoscale meteorology. Atmos. Chem. Phys. 13, 1395–1410. https://doi.org/10.5194/acp-13-1395-2013.
Pio, C.A., Ramos, M.M., Duarte, A.C., 1998. Atmospheric aerosol and soiling of external surfaces in an urban environment. Atmos. Environ. 32, 1979–1989. https://doi.org/10.1016/S1352-2310(97)00507-4.
Pope III, C.A., 2007. Mortality effects of longer term exposures to fine particulate air pollution: review of recent epidemiological evidence. Inhal. Toxicol. 19, 33–38. https://doi.org/10.1080/08958370701492961.
Querol, X., Alastuey, A., Rodríguez, S., Plana, F., Ruiz, C.R., Cots, N., Massagué, G., Puig, O., 2001. PM10 and PM2.5 source apportionment in the Barcelona metropolitan area, Catalonia Spain. Atmos. Environ. 35, 6407–6419. https://doi.org/10.1016/S1352-2310(01)00361-2.
PRTR, 2016. Spanish Register of Emissions and Pollutant Sources. Ministerio para la transición ecológica y el reto demográfico. https://bit.ly/2BzRArN. (Accessed 7 July 2017).
Querol, X., Alastuey, A., de la Rosa, J.D., Sánchez dela Campa, A., Plana, F., Ruiz, C.R., 2002. Source apportionment analysis of atmospheric particulates in an industrialised urban site in southwestern Spain. Atmos. Environ. 36, 3113–3125. https://doi.org/10.1016/S1352-2310(02)00257-1.
Querol, X., Alastuey, A., Moreno, T., Viana, M.M., Castillo, S., Pey, J., Rodríguez, S., Artiñano, B., Salvador, P., Sánchez, M., García Dos Santos, S., Herce Garraleta, M.D., Fernández-Partier, R., Moreno-Grau, S., Negral, L., Minguillón, M.C., Monfort, E., Sanz, M.J., Palomo-Marín, R., Pinilla-Gil, E., Cuevas, E., de la Rosa, J., Sánchez de la Campa, A.M., 2008. Spatial and temporal variations in airborne particulate matter (PM10 and PM2.5) across Spain 1999–2005. Atmos. Environ. 42, 3964–3979. https://doi.org/10.1016/j.atmosenv.2006.10.071.
Querol, X., Viana, M., Moreno, T., Alastuey, A. (Eds.), 2012. Bases científico-técnicas para un Plan Nacional de Mejora de la Calidad del Aire. CSIC.
Sánchez de la Campa, A.M., Sánchez-Rodas, D., Alsioufi, L., Alastuey, A., Querol, X., Jesús, D., 2018. Air quality trends in an industrialised area of SW Spain. J. Clean. Prod. 186, 465–474. https://doi.org/10.1016/j.jclepro.2018.03.122.
Sánchez-Rodas, D., Sánchez de la Campa, A., Oliveira, V., de la Rosa, J., 2012. Health implications of the distribution of arsenic species in airborne particulate matter. J. Inorg. Biochem. 108, 112–114. https://doi.org/10.1016/j.jinorgbio.2011.11.023.
Sen, P.K., 1968. Estimates of regression coefficient based on Kendall's tau. J. Am. Stat. Assoc. 63, 1379–1389. https://doi.org/10.1080/01621459.1968.10480934.
Stein, A.F., Draxler, R.R., Rolph, G.D., Stunder, B.J.B., Cohen, M.D., Ngan, F., 2015. NOAA's HYSPLIT atmospheric transport and dispersion modelling system. Bull. Am. Meteorol. Soc. 96, 2059–2077. https://doi.org/10.1175/BAMS-D-14-00110.1.
Theil, H., 1950. A rank invariant method of linear and polynomial regression analysis, I, II, III. Ned. Akad. Wentsch Proc. 53, 386–392. https://doi.org/10.1007/978-94-011-2546-8_20, 521–525 and 1397–1412.
Torres, R., Sánchez de la Campa, A.M., Beltrán, M., Sánchez-Rodas, D., de la Rosa, J.D., 2017. Geochemical anomalies of household dust in an industrialized city (Huelva, SW Spain). Sci. Total Environ. 587–588, 476–481. https://doi.org/10.1016/j.scitotenv.2017.02.167.
UNE-EN 12341, 2015. Standard Gravimetric Measurement Method for Determination of the PM10 or PM2.5 Mass Concentration of Suspended Particulate Matter.
Viana, M., Querol, X., Alastuey, A., Cuevas, E., Rodríguez, S., 2002. Influence of African dust on the levels of atmospheric particulates in the Canary Islands air quality network. Atmos. Environ. 36, 5751–5875. https://doi.org/10.1016/S1352-2310(02)00463-6.
Viana, M., Kuhlbusch, T., Querol, X., Alastuey, A., Harrison, R., Hopke, P., Winiwarter, W., Vallius, M., Szidat, S., Prévôt, A., Hueglin, C., Bloemen, H., Wåhlin, P., Vecchi, R., Miranda, A., KaspereGiebl, A., Maenhaut, W., Hitzenberger, R., 2008a. Source apportionment of particulate matter in Europe: a review of methods and results. J. Aerosol Sci. 39, 827–849. https://doi.org/10.1016/j.jaerosci.2008.05.007.
Viana, M., Pandolfi, M., Minguillón, M.C., Querol, X., Alastuey, A., Monfort, E., Celades, I., 2008b. Inter-comparison of receptor models for PM source apportionment: case study in an industrial area. Atmos. Environ. 42, 3820–3832. https://doi.org/10.1016/j.atmosenv.2007.12.056.

Environmental Pollution 290 (2021) 118065

Contents lists available at ScienceDirect

Environmental Pollution

journal homepage: www.elsevier.com/locate/envpol

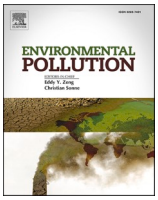

Contribution of anthropogenic and natural sources in PM10 during North African dust events in Southern Europe☆

María Millán-Martínez [a,b,*], Daniel Sánchez-Rodas [a,b], Ana M. Sánchez de la Campa [a,c], Jesús de la Rosa [a,d]

[a] Associate Unit CSIC-University of Huelva "Atmospheric Pollution", Center for Research in Sustainable Chemistry - CIQSO, University of Huelva, E21071, Huelva, Spain
[b] Department of Chemistry, Faculty of Experimental Sciences, University of Huelva, Campus El Carmen s/n, 21071, Huelva, Spain
[c] Department of Mining, Mechanic, Energetic and Construction Engineering, ETSI, University of Huelva, 21071, Huelva, Spain
[d] Department of Earth Science, Faculty of Experimental Sciences, University of Huelva, Campus El Carmen s/n, 21071, Huelva, Spain

ARTICLE INFO

Keywords:
PM10
North African dust
Source contribution
Southern Europe

ABSTRACT

The influence of North African (NAF) dust events on the air quality at the regional level (12 representative monitoring stations) in Southern Europe during a long time series (2007–2014) was studied. PM10 levels and chemical composition were separated by Atlantic (ATL) and NAF air masses. An increase in the average PM10 concentrations was observed on sampling days with NAF dust influence (42 μg m^{-3}) when compared to ATL air masses (29 μg m^{-3}). Major compounds such as crustal components and secondary inorganic compounds (SIC), as well as toxic trace elements derived from industrial emissions, also showed higher concentrations of NAF events. A source contribution analysis using positive matrix factorisation (PMF) 5.0 of the PM10 chemical data, discriminating ATL and NAF air mass origins, allowed the identification of five sources: crustal, sea salt, traffic, regional, and industrial. A higher contribution (74%) of the natural sources to PM10 concentrations was confirmed under NAF episodes compared with ATL. Furthermore, there was an increase in anthropogenic sources during these events (51%), indicating the important influence of the NAF air masses on these sources. The results of this study highlight that environmental managers should take appropriate actions to reduce local emissions during NAF events to ensure good air quality.

1. Introduction

Mineral dust is one of the main components of atmospheric particulate matter (PM). Large loads of mineral particles are transported from arid areas, contributing to different effects on climate, human health, and the environment (Towhy et al., 2009; Mahowald et al., 2010; Zhang et al., 2016; Middleton, 2019). The main global dust source regions are Central Asia, the Middle East, and North Africa, with the last region accounting for 55% of global dust emissions (Ginoux et al., 2010). Some authors have reported that dust coming from the Sahara desert can be transported to the Atlantic Islands and the Caribbean Sea (Prospero, 1999; Mahowald et al., 2005), and Southern Europe (Rodríguez et al., 2011; Salvador et al., 2019). PM levels are often increased as a consequence of these dust outbreaks (Viana et al., 2002; Querol et al., 2009; Salvador et al., 2013). In the case of Europe, the current Directive (EU, 2008) establishes an annual limit PM10 value (40 μg m^{-3}) as well as a daily limit value (50 μg m^{-3}, with a maximum of 35 days of exceedances). Furthermore, a procedure was developed to calculate the North African (NAF) load of the daily PM10 value when these events occur. For this purpose, PM10 background regional levels were calculated by applying either the 30th percentile (Escudero et al., 2007) or the 40th percentile to PM10 time series at regional background stations, after extracting the data associated with NAF dust outbreaks. Subsequently, the net African dust loads were obtained by subtracting the PM10 regional background levels from the PM10 values measured at the regional background sites during the NAF episodes. The European Directive 2008/50/EC (EU, 2008) allows the discount of PM exceedances due to NAF dust events.

From a global perspective, natural sources, such as NAF events, are more frequent than anthropogenic PM emissions. However,

☆ This paper has been recommended for acceptance by Prof. Pavlos Kassomenos.

* Corresponding author. Associate Unit CSIC-University of Huelva "Atmospheric Pollution", Center for Research in Sustainable Chemistry - CIQSO, University of Huelva, E21071, Huelva, Spain.
E-mail address: maria.millan@dqcm.uhu.es (M. Millán-Martínez).

https://doi.org/10.1016/j.envpol.2021.118065
Received 15 June 2021; Received in revised form 6 August 2021; Accepted 26 August 2021
Available online 28 August 2021

anthropogenic sources are important in several urban and industrial backgrounds in Spain (Rodríguez et al., 2007; Querol et al., 2008; Pandolfi et al., 2011). These emissions, mainly derived from traffic, industrial activities, and biomass burning, can release toxic elements and compounds, resulting in health problems for the local population (Galindo et al., 2018; Tobías et al., 2018). Recent studies have emphasised the negative health effects of NAF events (Pérez et al., 2008; Tobías et al., 2011; Pandolfi et al., 2014; Querol et al., 2019). In addition to the fact that higher coarse PM concentrations pose a risk to the human respiratory system, there is also a synergic effect between natural and anthropogenic pollutants. This dust transport brings about a PM concentration change, as well as a different air chemical composition (Pérez et al., 2012). Some authors have reported the adverse effects of NAF dust on regional pollutants, for example, the planetary boundary layer (PBL) is reduced when dust outbreaks occur (Pandolfi et al., 2014), causing the accumulation of anthropogenic pollutants. Furthermore, emissions from petrochemical activities or maritime transport are frequently co-transported with desert dust (Querol et al., 2019). Epidemiological studies have demonstrated an increase in daily mortality due to cardiovascular and respiratory diseases when Saharan dust events occur (Pérez et al., 2008; Sajani et al., 2011; Jiménez et al., 2010). Considering that North African dust transport has a strong impact on the Mediterranean basin (Pey et al., 2013; Salvador et al., 2014; Cabello et al., 2016), it is of great interest to determine how NAF dust affects PM levels and their different sources in the area.

The purpose of this study was to perform a PM10 source contribution analysis of natural and anthropogenic emissions under the influence of North African dust events in a large region (Andalusia) in Southern Europe. To this end, PM10 levels and their chemical components were studied at 12 monitoring stations (rural, urban, urban-industrial, and hot-spot traffic) belonging to the air quality monitoring network of the Autonomous Government of Andalusia during the period 2007–2014. Furthermore, a PMF analysis of the PM10 chemical composition was carried out considering the air mass origin during the sampling days to compare the source contribution.

2. Methodology

2.1. Study area

Andalusia is the southernmost autonomous community of mainland Spain and is the only European region with coastlines on both the Mediterranean and Atlantic oceans, which meets with the African continent through the Strait of Gibraltar. The main topography ranges of Andalusia are shown in Fig. 1, with the two most important mountain ranges in the north and the Baetic Range in the south. The Guadalquivir basin lies between these two mountainous areas. In general, the climate is typically the Mediterranean, with dry and hot summers and mild winters. There is a climatic variety with less wet weather in the eastern area of Andalusia. Higher rainfall is found from north to south as the sea is closer. Even though annual temperatures are not lower than 15 °C, they can vary depending on the altitude and continental characteristics of the considered area. Due to its proximity to North Africa, Andalusia is also affected by the impact of desert air masses, which increases PM concentrations (Rodríguez et al., 2001; Cachorro et al., 2008; Fernández-Camacho et al., 2010).

Although Andalusia is traditionally an agricultural area, the service sector (especially tourism) has grown in recent decades. Furthermore, deficient public transport results in dense urban road traffic and, consequently, road dust emissions (Amato et al., 2014; Milford et al., 2016). Likewise, although the industrial sector represents a minor percentage of the local economy, there are two main areas highly industrialised in Andalusia, which have been extensively studied: Algeciras Bay and the Ria of Huelva (Millán-Martínez et al., 2021). Many authors have concluded that there is a high proportion of anthropogenic and natural mineral particles in PM10 (Querol et al., 2004; Querol et al., 2008; de la Rosa et al., 2010; Pandolfi et al., 2011; Sánchez de la Campa et al., 2018; Millán-Martínez et al., 2021).

PM10 concentrations and chemical composition databases were obtained during the period 2007–2014 at 12 monitoring stations distributed across Andalusia (South Spain, Fig. 1). The considered monitoring sites belong to the Air Quality Monitoring Network of the Regional Government of Andalusia and were selected considering their location (rural, urban, or industrial background), as well as the main

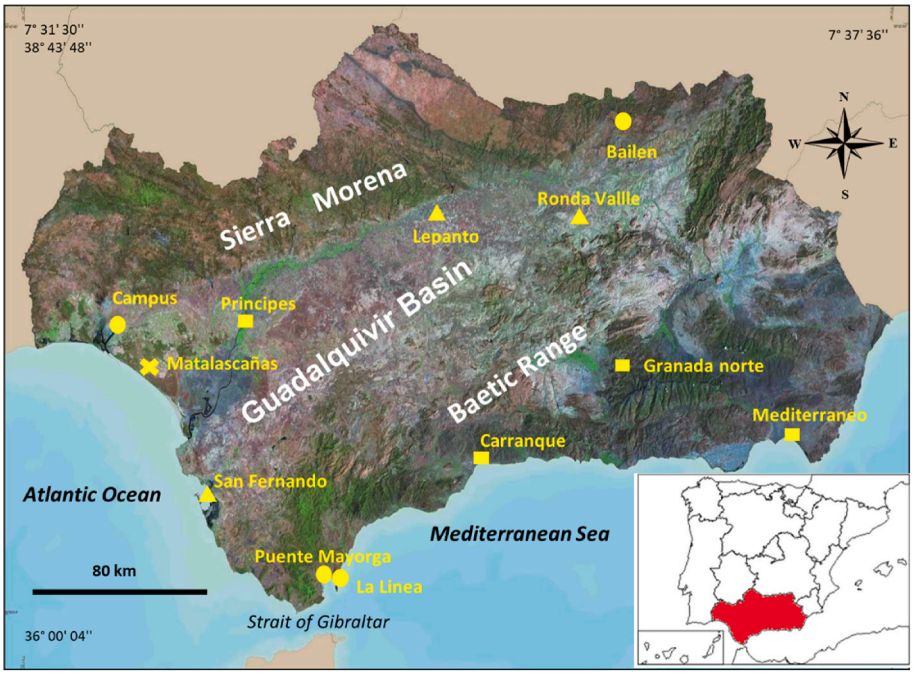

Fig. 1. Geographical location of the 12 monitoring stations considered in this study. Classification of the monitoring stations: traffic (square); urban-industrial (circle); urban (triangle); rural (cross).

nearby emission sources (Table S1):

1. Four traffic monitoring stations: Principes (Seville), Granada Norte, Carranque (Malaga), and Mediterraneo (Almeria).
2. Four urban-industrial monitoring stations: Campus (Huelva), La Linea (Cadiz), Puente Mayorga (Cadiz), and Bailen (Jaen).
3. Three urban monitoring stations, San Fernando (Cadiz), Ronda del Valle (Jaen), and Lepanto (Cordoba).
4. One rural monitoring station: Matalascañas (Huelva).

Principes and Granada Norte monitoring stations are located in the two most populated cities of Andalusia (Seville and Granada, respectively); hence, they are affected by dense urban traffic emissions (Fernández-Camacho et al., 2010; Sánchez-Rodas et al., 2017).

As previously mentioned, several monitoring stations are located in complex industrial areas. The campus is in the vicinity of the Huelva Estuary (Fig. 1), where industrial estates are established: a petrochemical complex, a phosphate industry for fertiliser production, and a Cu-smelter (Sánchez de la Campa et al., 2018). Previous studies in this area have reported sulfide-related toxic elements in PM (As, Cd, Sb, Bi, or Pb) as the main geochemical anomalies (Sánchez de la Campa et al., 2018; Millán-Martínez et al., 2021). In addition, one of the largest industrial estates of Andalusia is located close to the Strait of Gibraltar (Cadiz), which includes a petrochemical plant and oil refinery, a power plant, and a stainless-steel industry. Consequently, high levels of Ni, V, and Cr have been found at the monitoring stations in that area (La Linea and Puente Mayorga) as a result of this industrial activity, as well as the dense maritime traffic passing through the Strait of Gibraltar (Pandolfi et al., 2011; Li et al., 2018). The city of Bailen is one of the largest industrial estates producing structural ceramics in Spain, contributing to high levels of PM and SO_2 (Sánchez de la Campa et al., 2007; Sánchez de la Campa and de la Rosa, 2014).

The rural monitoring station of Matalascañas is located close to the coastal city of Huelva Matalascañas, within Doñana Natural Park and 30 km away from the industrial estates of Huelva.

2.2. PM10 sampling and chemical analysis

PM10 sampling was performed using quartz fibre filters (MUNKTELL) and high-volume captors (MCV: 30 $m^3\ h^{-1}$ and TISCH 68 $m^3\ h^{-1}$) following the normalised method UNE-EN 12341 (UNE, 2015). One daily sample (24 h) was collected every 6 days. The mass of PM10 retained on the filters was determined by the standard gravimetric procedures (temperature, 20 °C; relative humidity, 50%), employing a Sartorius LA130 S–F balance (0.1 mg sensitivity) (UNE, 2015). A total of 4793 daily samples were collected using the above procedure.

The analytical methodology used to determine PM10 chemical composition comprises several techniques, following the modified method proposed by Querol et al. (2002). A half fraction of each filter was acid digested (2.5 mL HNO_3: 5 mL HF: 2.5 mL $HClO_4$) for the analysis of major and trace elements by ICP-OES (Jobin Yvon model ULTIMA2) and ICP-MS (Agilent model 7700), respectively. For quality control, analysis of the NIST-1633b (fly ash, Standard Reference Material) was carried out during every analytical run of both ICP techniques. The digestion procedure of the PM samples and ICP analysis was also validated using the Standard Reference Material 1648a. External calibration was performed by ICP-MS using 1, 2, and 4 SPEX CertiPrep Claritas PPT® multielement solutions (1–250 $\mu g\ L^{-1}$ as well as HNO_3 5% blank). To minimise the possible fluctuations in the plasma, ^{103}Rh was used as an internal standard. The external calibration for ICP-OES was performed using elemental standard solutions (0.05–100 mg L^{-1} and HNO_3 5% blank). Accuracy and precision ranged from 5 to 10% for the elements studied.

Another quarter of the filter was leached with Milli-Q grade deionised water to extract water-soluble ions (SO_4^{2-}, NO_3^-, Cl^-, and NH_4^+) for subsequent analysis by ion chromatography (Methrom 883 Basic IC Plus) (Querol et al., 2002). The quality control of the results for soluble water ions was determined by solution cocktails for a low and high range of cations (1–10 mg L^{-1}) and anions (0.05–2.5 and 0.5–50 mg L^{-1}). The accuracy and detection limit for IC were 10% and 0.4 $\mu g\ m^{-3}$, respectively. Finally, a portion of 19.6 cm^2 of each filter was used for the analysis of the total carbon (TC) with a LECO SC-144 DR instrument.

SiO_2 and CO_3^{2-} concentrations were indirectly calculated from the stoichiometry of Al, Ca, and Mg-based on the experimental equation established by Querol et al. (2002): ($3*Al_2O_3 = SiO_2$; $1.5*Ca + 2.5*Mg = CO_3^{2-}$). $SO_4^{2-}{}_{\text{non-sea salt}}$ was obtained by subtracting the $SO_4^{2-}{}_{\text{sea salt}}$ (indirectly calculated by stoichiometry from the soluble Na levels) from the $SO_4^{2-}{}_{\text{total}}$. On average, 75%–86% and 67%–82% (for NAF and ATL, respectively) of PM mass were determined after analysing the collected filters.

2.3. Statistical treatment and source contribution

The chemical speciation data of the collected daily PM10 samples were used within the PMF (v5.0 EPA) for source identification and apportionment. The PMF model is a factor analytical tool used to calculate the contributions and chemical profiles of the sources developed by Paatero and Tapper (1994) and Paatero (1997). The PMF is based on the following mathematical algorithm:

$$\chi_{ij} = \sum_{k-1}^{p} g_{ik} * f_{kj} + e_{ij}$$

The dataset can be expressed as a matrix x of i by j dimensions, where i is the number of samples and j is the measured chemical elements, p is the number of independent factors, g_{ik} is the amount of mass contributed by each factor for each sample, f_{kj} represents the species profiles of each factor, and e_{ij} is the residue for each sample by element.

PMF is a weighted least-squares method in which individual estimates of the uncertainty in each data value need to be included in the input matrix. Several sources of error contribute to measurement uncertainty, but the associated with the analytical procedure is probably one of the most important. The uncertainties were calculated according to the methodology proposed by Amato et al. (2009).

Elements were classified using the signal-to-noise ratio defined by Paatero and Hopke (2003). Elements with S/N < 2 were generally defined as weak variables. The only common weak element at all the monitoring stations was As, although other sulfide-like trace elements such as Zn or Bi also appeared to be weak in some of the sites. Because the S/N ratio is very sensitive to sporadic values much higher than the level of noise, the percentage of data above the detection limit was used as a complementary criterion.

2.4. Air masses origin

The origin of air masses affecting the monitoring stations for each sampling day was determined by considering two representative locations: western Andalusia (37° N, 6° W) and Eastern Andalusia (37° N, 3° W). To this end, a five-day back-trajectory analysis starting at three different altitudes (500, 1500, and 2500 m a. s. l.) was carried out using the HYSPLIT model (Stein et al., 2015) of the NOAA Air Resources Laboratory (ARL) (https://www.ready.noaa.gov/HYSPLIT.php). Additionally, NAF events affecting the monitoring stations were also studied using aerosol and dust maps and satellite images from NRL (http://www.nrlmry.navy.mil/aerosol), SKIRON (https://forecast.uoa.gr/en/forecast-maps/dust/north-atlantic), BSC DUST (https://ess.bsc.es/bsc-dust-daily-forecast), and Earth Data NASA project (https://worldview.earthdata.nasa.gov/).

We classified the daily air masses as North African (NAF) when an African dust outbreak occurs, and the Atlantic (ATL), including the one from N, NW, SW, and W Atlantic air masses. There are also other minor air masses (regional, Mediterranean, and European origins <5%).

During the study period (2007–2014) NAF represented 26% and 31% of the total for Western and Eastern Andalusia, respectively (Fig. S1). The occurrence of NAF air masses is more frequent between March and September and is especially significant during the summer months (Fig. S2).

3. Results and discussion

3.1. Chemical composition of PM10

The interannual mean PM10 levels measured in Andalusia for the period 2007–2014 ranged from 28 μg m^{-3} (rural), 23–30 μg m^{-3} (urban), 32–36 μg m^{-3} (urban-industrial)–33-40 μg m^{-3} (traffic) (Fig. 2). PM10 concentration generally decreased in every type of monitoring station compared to previous data in the same study area. For example, de la Rosa et al. (2010) reported higher values (31–32, 35–53, 31–62 and 54–63 μg m^{-3} at rural, urban, urban-industrial, and traffic monitoring sites, respectively) in 2007. At the Bailen monitoring site, a PM10 concentration of 57.7 μg m^{-3} was obtained during the period 2003–2008 (Sánchez de la Campa et al., 2014). Furthermore, 41 and 44 μg·PM10 m^{-3} were observed at Principes and Granada Norte, respectively, from 2007 to 2010 (Amato et al., 2014). The same decreasing trend in PM10 concentration was observed at the industrial estates of La Linea and Puente Mayorga for the period 2005–2007 (37 and 38 μg m^{-3} Li et al., 2018) and at Campus site (37 μg m^{-3} for the period 2001–2008) (Sánchez de la Campa et al., 2018). All these studies conclude that the implementation of industrial emission abatement systems and the application of European directives on air quality are the main reasons to obtain lower PM10 concentrations. Fig. 2 shows that the maximum mean PM10 concentrations at the regional level were always associated with NAF episodes compared to ATL air mass origin, which has been observed in many other studies in Spain and the Mediterranean basin (Querol et al., 2019; Salvador et al., 2019; Conte et al., 2020).

3.1.1. Major components

The contribution of the major components to PM10 for each type of monitoring station for the NAF and ATL air masses is shown in Fig. 3. Higher mean concentrations of crustal components (CO_3^{2-} Al_2O_3, SiO_2, Fe, Ca, K, Fe, and P) were found in traffic sites (Granada Norte, Principes, Carranque, and Mediterraneo), reaching 34 %–42% of the PM10 mass. However, the mean concentrations observed under the influence of NAF (20.4 μg m^{-3}) were almost twice the mineral dust concentration for ATL air masses (11.4 μg m^{-3}). Lower concentrations (11.4–15.0 μg m^{-3} and 7.2–8.6 μg m^{-3} for NAF and ATL air masses, respectively) were obtained for the urban-industrial background, except for Bailen (24.7 and 12.2 μg m^{-3} for NAF and ATL, respectively), related to a relevant ceramic industrial activity (Sánchez de la Campa and de la Rosa, 2014).

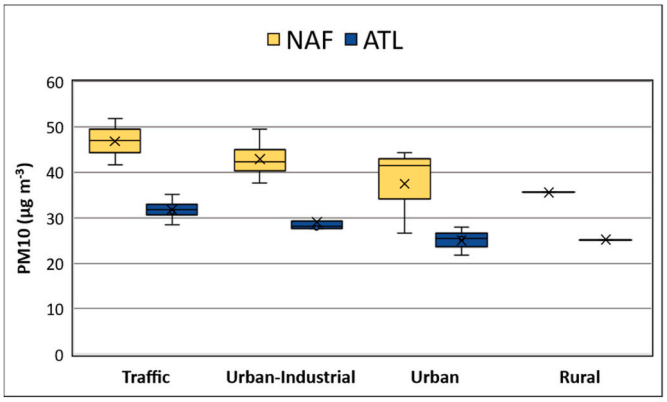

Fig. 2. Whisker and box plot of PM10 concentrations measured at the monitoring stations of Andalusia during the period (2007–2014) under NAF and ATL air masses.

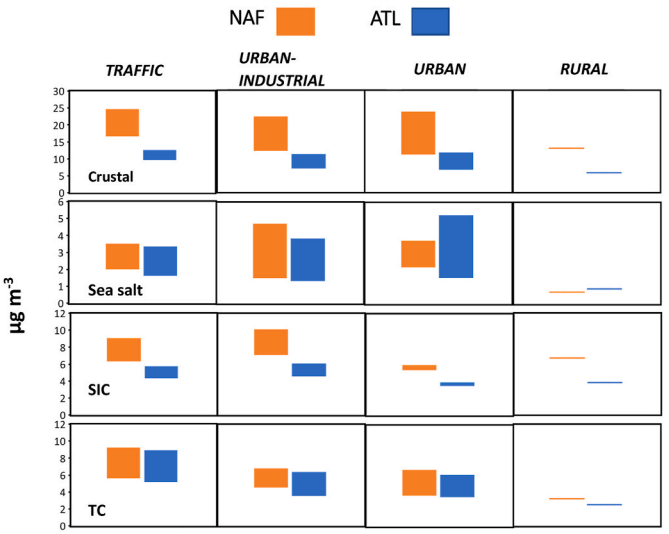

Fig. 3. Mean ranges of PM10 major components (μg·m^{-3}) measured at the monitoring stations of Andalusia under NAF and ATL air masses origin.

For urban monitoring stations, the mineral contribution ranged between 9.3 and 19.8 μg m^{-3} during NAF events, compared to the interval 5.6–9.8 μg m^{-3} registered under ATL influence. The mean concentration observed in the rural station (Matalascañas) during NAF episodes (13.0 μg m^{-3}) was more than twice that obtained during ATL air masses (5.8 μg m^{-3}). More marked concentration differences were observed at the stations (Granada Norte, Bailen, and Ronda Valle) with important local sources, mainly industrial or traffic. These monitoring sites are located in Eastern Andalusia, at higher altitudes, where the NAF air mass frequencies are higher. In conclusion, the differences between NAF and ATL samples could be due to several factors, such as site typology, local sources, and monitoring station altitude.

Regarding secondary inorganic compounds (SIC: NO_3^-, $SO_4^{2-}{}_{non\text{-}sea\ salt}$ and NH_4^+), high mean concentrations were found at the industrial monitoring stations as is expected due to the anthropogenic SO_4^{2-} emissions from fuel oil combustion. A remarkable decrease in SIC concentrations compared to earlier periods was observed (e.g. 10 μg·SIC m^{-3}, Amato et al., 2014). The higher mean concentrations obtained under NAF air masses of these anthropogenic compounds (8.7 μg m^{-3}) in comparison to the ATL air masses (5.4 μg m^{-3}). At the traffic sites, the concentrations found were similar to those measured at the industrial monitoring stations, with a mean value of 7.7 μg m^{-3} for NAF air masses and 5.1 μg m^{-3} for ATL influence. Lower mean concentrations were observed at urban (5.5 and 3.8 μg m^{-3} for NAF and ATL air masses, respectively) and rural (6.7 and 3.8 μg m^{-3} for NAF and ATL air masses, respectively).

The mean contribution of sea salt aerosol reached higher values at urban-industrial and rural monitoring stations (3.1–4.6 μg m^{-3}), coinciding with most of the coastal sites of the study. No significant differences were observed between the NAF and ATL air masses. The mean concentrations of TC under NAF air masses increased from 3.3 μg m^{-3} in rural background stations, to 5.4 and 5.6 μg m^{-3} in urban and urban-industrial sites, respectively. The highest mean concentration (7.2 μg m^{-3}) corresponded to traffic sites in relation to vehicle exhaust emissions. Furthermore, high levels of carbonaceous particles were also observed in Bailen, in agreement with previously published results (Sánchez de la Campa and de la Rosa, 2014). In this industrial estate, coke, olive husks, and wood are used as fuels for structural ceramic manufacturing (Sánchez de la Campa et al., 2010).

From these results concerning the crustal components, SIC and TC, it can be concluded that higher concentrations were always found under NAF events compared to ATL air masses origin, as has also been previously observed for PM10 concentrations.

3.1.2. Trace elements

The mean interannual concentrations of representative trace elements in PM10 were studied individually for each monitoring site (Fig. S3). The highest level of As was found in Campus, which was derived from nearby Cu-smelter emissions (Sánchez de la Campa et al., 2018). The difference of mean As concentrations between ATL (4.3 ng m^{-3}) and NAF (7.2 ng m^{-3}) air masses is remarkable, exceeding, in this case, the European annual target value (6 ng m^{-3}), which does not take into account synoptic scenarios and air masses origin. In the case of the Campus monitoring station, these results suggest that during NAF events, there is an increase in As concentrations favoured by their coupling with industrial plumes (Fernández-Camacho et al., 2010). In this monitoring station, it is also noteworthy that the mean levels of Cu (64.2 ng m^{-3}), Zn (63 ng m^{-3}), Pb (16.3 ng m^{-3}), Cd (0.76 ng m^{-3}), and Bi (0.96 ng m^{-3}) under NAF influence, originated from the Cu-smelter activities. However, concerning the elements with annual target values in the EU Normative, air quality thresholds were not exceeded (500 ng Pb·m^{-3}, EU, 2008; 5 ng Cd·m^{-3}; EU, 2004) in Huelva.

Lepanto is characterised by high mean levels of Cu and Zn (105 and 219 ng m^{-3}, respectively, for NAF episodes) as a result of nearby smelters of these metals. Another example of high concentrations of Cu was found in Bailen (137 ng m^{-3} under NAF) and was related to a nearby ceramic industry (Sánchez de la Campa et al., 2014).

V and Ni are other tracers of industrial activity linked to ship traffic emissions and petrochemical activities (Moreno et al., 2006). High mean Ni concentrations were observed in the Strait of Gibraltar (La Linea and Puente Mayorga), showing similar concentrations of NAF and ATL masses (14–18 ng m^{-3}) (Fig. S3), although the European limit did not exceed (EU, 2004). Levels of V also showed high mean values in these industrial monitoring sites, especially during NAF episodes (36.2 and

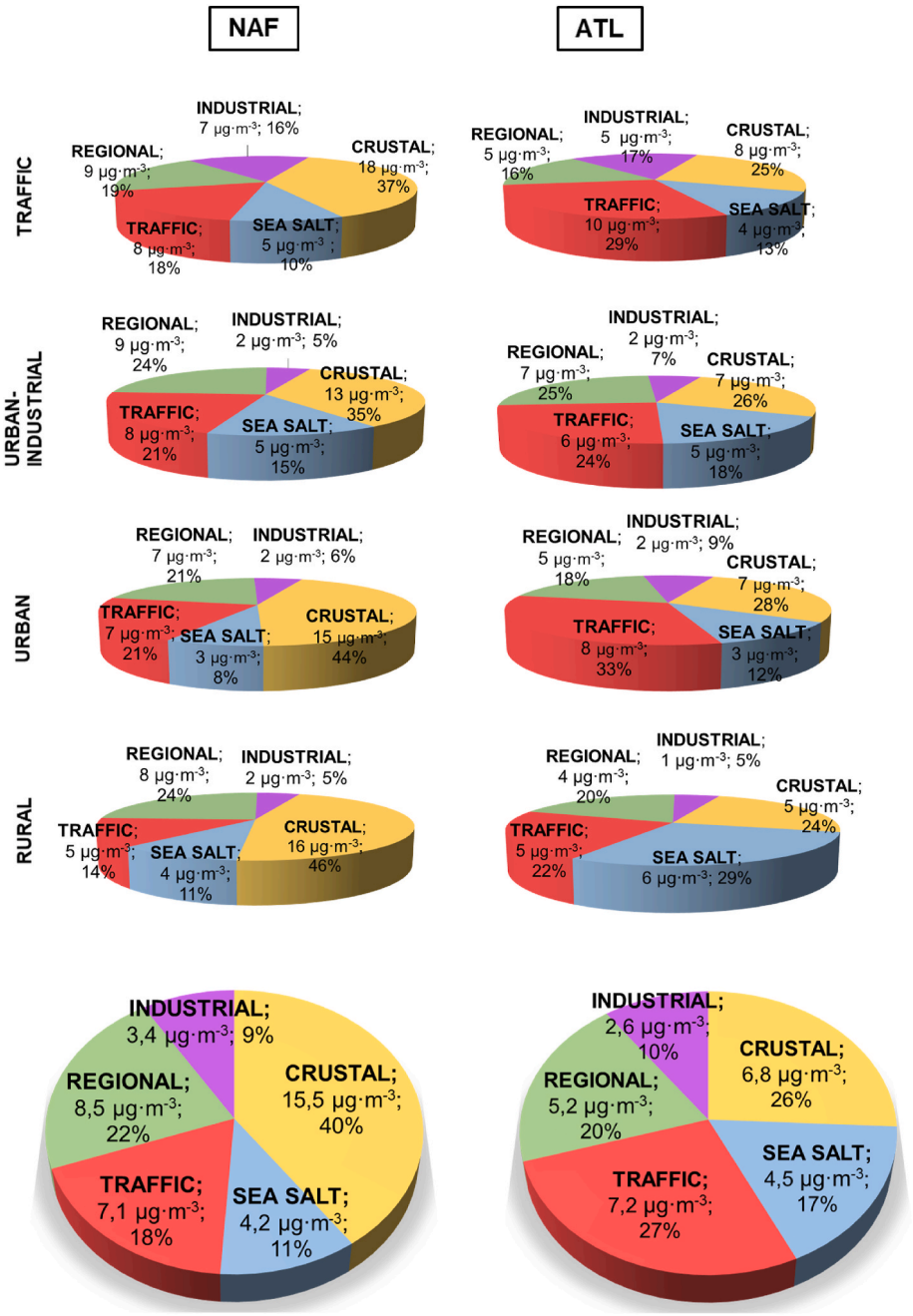

Fig. 4. Pie charts of average source contribution (µg m^{-3}, %) to PM10 for the selected monitoring stations under NAF and ATL air masses.

31.9 ng m^{-3} at Puente Mayorga and La Linea, respectively). (Fig. S3). Rodríguez et al. (2011) reported the presence of V in desert dust as a consequence of industrial emissions from North Africa. Furthermore, as has been previously observed (Sánchez de la Campa et al., 2014), the coke used as fuel in brick factories in Bailen resulted in high V concentrations (33.5 ng m^{-3} in NAF air masses).

Maximum values of mean Cr concentrations were registered at La Linea and Puente Mayorga (8.5 and 8.9 ng m^{-3}, respectively for NAF), derived from the industrial activity of a stainless-steel factory. In this case, Cr concentrations under ATL air masses (11.9 and 10.9 ng m^{-3} at La Linea and Puente Mayorga, respectively) are higher because of the dominant westerly wind in the area (Pandolfi et al., 2011). Likewise, this metal can be found in high concentrations (5.9 ng m^{-3} for NAF) in Granada Norte, and is derived from heavy traffic. The hot-spot traffic monitoring sites considered in this work showed the highest mean concentrations of Sn and Sb and trace elements related to brake and tyre wear. Average Sn and Sb levels found at Granada Norte during NAF episodes were 5.2 and 4.1 ng m^{-3}, respectively. In addition, the non-exhaust vehicle emissions caused high mean concentrations of Cu and Cr (approximately 60 and 5 ng m^{-3}, respectively) in the traffic sites.

3.2. Source contribution analysis (NAF vs ATL)

Following the PMF model described above, a source apportionment analysis using PMF 5.0 was performed to identify and quantify the natural and anthropogenic sources contributing to PM10 at every monitoring station during the period 2007–2014. Fig. 4 shows the different sources determined by considering the two main air masses originating in the study area, NAF and ATL.

The contribution of the sources is highly defined by the type and location of the monitoring stations. Nevertheless, the majority of them have the contribution of two main groups of sources in common: natural (crustal and sea salt) and anthropogenic (traffic, regional, and industrial).

The **crustal source** showed typical silicate components, such as Al_2O_3, Fe, Ca, Rb, Ti, Mn, and Sr. These soil-like elements are mainly derived from local dust resuspension and long-range transport of North African dust. As expected for an area close to the sea, a **sea salt** source was also identified with the characteristic marine elements Na, Cl, and Mg.

The **traffic source** was characterised by high concentrations of NO_3^-, NH_4^+, and total carbon (TC) due to vehicle exhaust emissions. Furthermore, high concentrations of Sn, Sb, Cu, Zn, K, Ca, and Ti were also found within this source, originating from the non-exhaust vehicle emissions (brake and tyre wear and road dust resuspension) (Amato et al., 2014).

Another source found in all monitoring sites was a **regional** one, with SO_4^{2-}, NO_3^-, and NH_4^+ as typical components. These components are normally associated with emissions from petrochemical activities or maritime transport, characterised by high concentrations of Ni, V, Co, Sn, Pb, Sb, Cr, and Mn. Moreover, an **industrial** source was identified in some of the monitoring stations with a specific chemical profile determined by nearby industrial activities.

Table 1 summarises the average source contribution of the selected monitoring stations under NAF and ATL air masses. Concerning the crustal source, a higher mean contribution under NAF (15 μg m^{-3}) influence compared to ATL (6 μg m^{-3}) air masses (Fig. 4), as a consequence of the mineral components coming from the desert dust, has been observed. Maximum mean concentrations of the crustal source were obtained at the hot-spot traffic sites (19.1 and 19.8 at Granada Norte and Carranque under NAF events, respectively) (Table 1). These high values, derived from the road dust resuspension coupled to NAF dust, are in the range observed in previous works in the Mediterranean basin (Querol et al., 2008; Pandolfi et al., 2016). In general, the concentration of the sea salt source was higher at the coastal monitoring stations with a similar contribution under NAF and ATL events (4 and 5 μg m^{-3}, respectively).

The same mean contribution of the traffic source was found for NAF and ATL (7 μg m^{-3}) in most of the monitoring sites. This fact was also observed in Principes (Fernández-Camacho et al., 2016), and can be attributed to the fine particulate fraction origin of the traffic-related compounds (Amato et al., 2014). It is also worth noting that NAF events normally occur during warmer seasons, whereas traffic sources always increase their contribution during the winter (Cesari et al., 2018; Mazzei et al., 2008). Furthermore, in some monitoring sites, this source was mixed with biomass combustion (with K as the main tracer) (Alves et al., 2011).

Regarding the regional source, derived mainly from long-range anthropogenic emissions, contributions were almost twice under NAF events in most of the monitoring stations (Table 1). A mean concentration of 8 μg m^{-3} was obtained for NAF air masses in comparison to ATL (5 μg m^{-3}), within the range described in other Southern European cities (Amato et al., 2014; Cesari et al., 2018), although no difference between NAF and ATL air masses has been found in these studies.

Different industrial sources were identified according to the industrial activity developed in the area surrounding each monitoring station.

Table 1
Mean source contribution (μg m^{-3}) to PM10 levels at the monitoring stations of Andalusia under North African (N) and Atlantic (A) air masses during the period 2007–2014.

Monitoring station	Natural Sources μg m^{-3} *(%)*				Anthropogenic sources μg m^{-3} *(%)*					
Traffic	Crustal		Sea salt		Traffic		Regional		Industrial	
	NAF	ATL	NAF	ATL	NAF	ATL	NAF	ATL	NAF	ATL
Granada Norte	19.1 *(39)*	5.1 *(16)*	2.6 *(5)*	2.0 *(16)*	14.8 *(30)*[a]	17.1 *(51)*[a]	12.6 *(26)*	8.8 *(27)*	–	–
Principes	15.4 *(35)*	6.8 *(23)*	3.9 *(9)*	3.4 *(12)*	7.3 *(17)*	8.3 *(28)*	9.4 *(22)*	5.2 *(18)*	7.5 *(17)*	5.5 *(19)*
Carranque	19.8 *(49)*	11.6 *(42)*	8.3 *(21)*	5.9 *(21)*	6.2 *(15)*	6.3 *(23)*	6.2 *(15)*	4.1 *(14)*	–	–
Mediterraneo	16.6 *(50)*	9.7 *(38)*	4.1 *(12)*	5.4 *(22)*	4.9 *(15)*[a]	6.4 *(25)*[a]	7.9 *(23)*	3.7 *(15)*	–	–
Urban-Industrial										
Bailen	16.7 *(39)*	7.1 *(24)*	4.4 *(11)*	3.1 *(11)*	6.0 *(14)*	7.0 *(24)*	11.6 *(27)*[b]	9.4 *(32)*[b]	3.9 *(9)*	2.8 *(9)*
Campus	8.7 *(28)*	4.8 *(21)*	4.4 *(14)*	4.3 *(18)*	7.9 *(25)*[a]	8 *(34)*[a]	8.3 *(27)*	4.9 *(21)*	2.1 *(6)*	1.4 *(6)*
La Linea	12.6 *(34)*	7.7 *(29)*	4.5 *(12)*	4.6 *(18)*	11.1 *(29)*	5.0 *(19)*	8.4 *(22)*	7.2 *(28)*	1.1 *(3)*	1.5 *(6)*
Pte. Mayorga	13.9 *(37)*	8.0 *(29)*	8.5 *(22)*	7.0 *(26)*	6.8 *(18)*[a]	5.8 *(21)*[a]	7.6 *(20)*	5.3 *(19)*	1.0 *(3)*	1.3 *(5)*
Urban										
Ronda Valle	17.5 *(49)*	7 *(29)*	2.9 *(8)*	2.1 *(9)*	9.3 *(26)*	9.9 *(42)*	6.3 *(17)*[b]	4.7 *(20)*[b]	–	–
Lepanto	20.1*(48)*	8.6 *(33)*	1.4 *(3)*	1.2 *(1)*	7.4 *(18)*[b]	8.3 *(32)*[b]	10.8 *(26)*	5.6 *(22)*	2.1 *(5)*	2.1 *(8)*
San Fernando	8.9 *(37)*	5.2 *(26)*	4.4 *(18)*	5.5 *(28)*	5.3 *(23)*[a]	6.1 *(30)*[a]	5.1 *(22)*	3.3 *(16)*	–	–
Rural										
Matalascañas	15.9 *(46)*	5.0 *(24)*	3.7 *(11)*	6.2 *(29)*	4.7 *(14)*[a]	4.8 *(22)*[a]	8.5 *(24)*	4.2 *(20)*	1.8 *(5)*	1.1 *(5)*

[a] Traffic + Combustion.
[b] Regional + Combustion.

At the Bailen industrial site, a source characterised by high concentrations of V, Ni, Pb, and SO_4^{2-} was found. These components, derived from brick factory emissions (Sánchez de la Campa and de la Rosa, 2010), showed a contribution of 3.9 and 2.8 μg m^{-3} for NAF and ATL influence, respectively. Two industrial sources were observed at Campus. The first one, typified by Cu, Zn, As, Cd, and Pb, corresponds to the emissions from a Cu-smelter (Fernández-Camacho et al., 2010). Another industrial source is the production of phosphate derivatives, which has also been described by other authors (Querol et al., 2002; Alatuey et al., 2006; Fernández-Camacho et al., 2012). The sum of the two industrial sources contributed to PM10 mass 2.1 and 1.4 μg m^{-3} for NAF and ATL air masses, respectively. Even though Matalascañas is considered a rural site, an industrial source derived from the two industrial estates mentioned above at the Campus site was identified. This is due to the closeness (ca. 30 km) of the rural station to the industrial activity, representing a contribution of 2.0 and 1.0 μg m^{-3} under NAF and ATL air masses.

The two monitoring stations located near the Strait of Gibraltar (La Linea and Puente Mayorga) presented an industrial source characterised by high concentrations of Cr, Ni, Zn, Mn, Cd, and Pb, related to the metallurgical activity emissions (Li et al., 2018). In this case, a similar contribution of this source was observed under ATL air masses (1.5 and 1.3 μg m^{-3} at La Linea and Puente Mayorga, respectively) compared to NAF events (1.1 and 1.0 μg m^{-3}) related to dominant western winds in the area (Sánchez de la Campa et al., 2011).

Other monitoring stations with industrial sources are Principes traffic site due to local industrial emissions from detergent production (Fernández-Camacho et al., 2016); and the urban station of Lepanto, as a result of metallurgic-related activities developed close to the monitoring station (de la Rosa et al., 2010; Sánchez-Rodas et al., 2017).

The most significant difference between the studied air mass origins was observed in the average contribution of the crustal source (15.5 and 6.8 μg m^{-3} for NAF and ATL, respectively), corresponding to an increase of 128%. This has already been postulated as the main reason for the PM10 concentration difference (Rodríguez et al., 2011; Salvador et al., 2019). However, the higher contribution of some anthropogenic pollutants to NAF events is also remarkable. Even though the traffic pollutants kept similar concentrations under both air masses, an increase in the sum of regional and industrial sources when comparing NAF (11.8 μg m^{-3}) and ATL (7.8 μg m^{-3}) events was noticed, representing a difference of 51% (Fig. 3). This may suggest an influence of the dust coming from North Africa over the anthropogenic pollutants, in addition to the well-known mineral contribution of these events.

North African dust events are associated with an increased risk of mortality (Tobías et al., 2011; Pandolfi et al., 2014; Stafoggia et al., 2016). These dust episodes cause PBL reduction due to a pushing-down effect of the warm overlying African air masses, which changes the temperature profile and lowers the inversion (Pandolfi et al., 2013). Consequently, anthropogenic emissions tended to accumulate. The fine grain size origin of anthropogenic particle pollutants and their high concentration in toxic elements have harmful effects on the health of the population. Hence, environmental managers should take appropriate actions to reduce local emissions during NAF events to ensure good air quality.

4. Conclusions

The present study highlights the importance of performing long-term series studies of source contribution using chemical data of PM10 at the regional level in Southern Europe. Mean PM10 concentrations and their chemical composition were studied during the period from 2007 to 2014 to differentiate between two scenarios: NAF events and ATL air masses origin. The results showed an increase in the mean PM10 concentrations under the NAF episodes compared to the ATL air masses. Furthermore, SIC compounds and some toxic elements (As, V, Ni, Pb, and Bi) related to industrial emissions also presented higher mean concentrations under these dust events.

Two main groups of sources have been identified by PMF, considering the origin of NAF and ATL air masses: natural (crustal and sea salt) and anthropogenic (traffic, regional, and industrial). The crustal contribution represents a gain of 128% during the NAF air masses. In addition, there was also a significant increase (51%) in anthropogenic sources, suggesting an influence of the NAF events on local anthropogenic emissions. Therefore, it has been demonstrated at the regional level that dust coming from North Africa affects not only PM10 exceedances but also their chemical composition. The population could be especially exposed to more harmful air quality during these days, and hence, additional considerations should be taken to reduce the toxic anthropogenic pollution affecting human health.

Declaration of competing interest

The authors declare that they have no known competing financial interests or personal relationships that could have appeared to influence the work reported in this paper.

Acknowledgments

We would like to acknowledge the project of the Ministry of Science, Innovation, and Universities of Spain (Project RTI 2018-095937-B-I00) and the Environmental Agency of Andalusia for financial and technical support. Funding for open access charge: Universidad de Huelva / CBUA.

Appendix A. Supplementary data

Supplementary data to this article can be found online at https://doi.org/10.1016/j.envpol.2021.118065.

Sample Credit author statement

María Millán Martínez: Investigation, Writing Original Draft. Daniel Sánchez-Rodas: Reviewing, Methodology. Ana M. Sánchez de la Campa: Reviewing, Methodology. Jesús D. de la Rosa: Funding Acquisition, Reviewing.

References

Alastuey, A., Querol, X., Plana, F., Viana, M., Ruiz, C.R., Sánchez de la Campa, A.M., de la Rosa, J., Mantilla, E., García dos Santos, S., 2006. Identification and chemical characterization of industrial particulate matter sources in southwest Spain. J. Air Waste Manag. Assoc. 56, 993–1006. https://doi.org/10.1080/10473289.2006.10464502.

Alves, C., Goncalves, C., Fernandes, A.P., Tarelho, L., Pio, C., 2011. Fireplace and woodstove fine particle emissions from combustion of western Mediterranean wood types. Atmos. Res. 101, 692–700. https://doi.org/10.1016/j.atmosres.2011.04.015.

Amato, F., Pandolfi, M., Escrig, A., Querol, X., Alastuey, A., Pey, J., Perez, N., Hopke, P. K., 2009. Quantifying road dust resuspension in urban environment by multilinear engine: a comparison with PMF2. Atmos. Environ. 43, 2770–2780. https://doi.org/10.1016/j.atmosenv.2009.02.039.

Amato, F., Alastuey, A., de la Rosa, J., Gonzalez-Castanedo, Y., Sánchez de la Campa, A. M., Pandolfi, M., Lozano, A., Contreras González, J., Querol, X., 2014. Trends of road dust emissions contributions on ambient air particulate levels at rural, urban and industrial sites in southern Spain. Atmos. Chem. Phys. https://doi.org/10.5194/acp-14-3533-2014.

Cabello, M., Orza, J.A.G., Dueñas, C., Liger, E., Gordo, E., Cañete, S., 2016. Back-trajectory analysis of African dust outbreaks at a coastal city in southern Spain: selection of starting heights and assessment of African and concurrent Mediterranean contributions. Atmos. Environ. 140, 10–21. https://doi.org/10.1016/j.atmosenv.2016.05.047.

Cachorro, V.E., Toledano, C., Prats, N., Sorribas, M., Mogo, S., Berjon, A., Torres, B., Rodrigo, R., de la Rosa, J., De Frutos, A.M., 2008. The strongest desert dust intrusion mixed with smoke over the Iberian Peninsula registered with Sun photometry. J. Geophys. Res. 113, D14S04. https://doi.org/10.1029/2007JD009582.

Cesari, D., De Benedetto, G.E., Bonasoni, P., Busetto, M., Dinoi, A., Merico, E., Chirizzi, D., Cristofanelli, P., Donateo, A., Grasso, F.M., Marinoni, A., Pennetta, A., Contini, D., 2018. Seasonal variability of PM2.5 and PM10 composition and sources in an urban background site in Southern Italy. Sci. Total Environ. 612, 202–213. https://doi.org/10.1016/j.scitotenv.2017.08.230.

Conte, M., Merico, E., Cesari, D., Dinoi, A., Grasso, F.M., Donateo, A., Guascito, M.R., Contini, D., 2020. Long-term characterisation of African dust advection in south-eastern Italy: influence on fine and coarse particle concentrations, size distributions, and carbon content. Atmos. Res. 233, 10469–10490. https://doi.org/10.1016/j.atmosres.2019.104690.

de la Rosa, J.D., Sanchez de la Campa, A.M., Alastuey, A., Querol, X., Gonzalez-Castanedo, Y., Fernandez-Camacho, R., Stein, A.F., 2010. Using PM10 geochemical maps for defining the origin of atmospheric pollution in Andalusia (Southern Spain), Atmos. Environ. Times 44, 4595–4605. https://doi.org/10.1016/j.atmosenv.2010.08.009.

Escudero, M., Querol, X., Pey, J., Alastuey, A., Pérez, N., Ferreira, F., Alonso, S., Rodríguez, S., Cuevas, E., 2007. A methodology for the quantification of the net African dust load in air quality monitoring networks. Atmos. Environ. 41, 5516–5524. https://doi.org/10.1016/j.atmosenv.2007.04.047.

European Commission, 2004. Directive 2004/107/EC relating to arsenic, cadmium, mercury, nickel and polycyclic aromatic hydrocarbons in ambient air last accessed july 2017. https://bit.ly/2PQHh7W.

European Commission, 2008. Directive 2008/50/CE on ambient air quality and cleaner air for Europe last accesed july 2017. https://bit.ly/2R7Peu3.

Fernández-Camacho, R., de la Rosa, R., Sanchez de la Campa, A.M., González-Castañedo, Y., Alatuey, A., Querol, X., Rodríguez, S., 2010. Geochemical characterization of Cu-smelter emission plumes with impact in an urban area of SW Spain. Atmos. Res. 96, 590–601. https://doi.org/10.1016/j.atmosres.2010.01.008.

Fernández-Camacho, R., Rodríguez, S., de la Rosa, J.D., Sánchez de la Campa, A.M., Alastuey, A., Querol, X., González-Castanedo, Y., Garcia-Orellana, I., Nava, S., 2012. Ultrafine particle and fine trace metal (As, Cd, Cu, Pb and Zn) pollution episodes induced by industrial emissions in Huelva, SW Spain. Atmos. Environ. 61, 507–517. https://doi.org/10.1016/j.atmosenv.2012.08.003.

Fernández-Camacho, R., de la Rosa, J.D., Sánchez de la Campa, A.M., 2016. Trends and sources vs air mass origins in a major city in South-western Europe: implications for air quality management. Sci. Total Environ. 553, 305–315. https://doi.org/10.1016/j.scitotenv.2016.02.079.

Galindo, N., Yubero, E., Nicolás, J.F., Varea, M., Clemente, A., 2018. Day-night variability of PM10 components at a Mediterranean urban site during winter. Air Qual. Atmos. Health 11, 1251–1258. https://doi.org/10.1007/s11869-018-0627-8.

Ginoux, P., Prospero, J.M., Gill, T.E., Hsu, N.C., Zhao, M., 2010. Global-scale attribution of anthropogenic and natural dust sources and their emission rates based on MODIS Deep Blue aerosol products. Rev. Geophys. 50, 10875–10893. https://doi.org/10.1029/2012RG000388.

Jiménez, E., Linares, C., Martínez, D., Díaz, J., 2010. Role of Saharan dust in the relationship between particulate matter and short-term daily mortality among the elderly in Madrid (Spain). Sci. Total Environ. 408 (23), 5729–5736. https://doi.org/10.1016/j.scitotenv.2010.08.049.

Li, J., Chen, B., de la Campa A M, S., Alastuey, A., Querol, X., de la Rosa, J.D., 2018. 2005-2014 trends of PM10 source contributions in an industrialized area of southern Spain. Environ. Pollut. 236, 570–579. https://doi.org/10.1016/j.envpol.2018.01.101.

Mahowald, N.M., Baker, A.R., Bergametti, G., Brooks, N., Duce, R.A., Jickells, T.D., Kubilay, N., Prospero, J.M., Tegen, I., 2005. Atmospheric global dust cycle and iron inputs to the ocean. Global Biogeochem. Cycles 19, GB4030. https://doi.org/10.1029/2004GB002402.

Mahowald, N.M., Kloster, S., Engelstaedter, S., Moore, J.K., Mukhopadhyay, S., Mcconnell, J.R., Albani, S., Doney, S.C., Bhattacharya, A., Curran, M.a.J., Flanner, M.G., Hoffman, F.M., Lawrence, D.M., Lindsay, K., Mayewski, P.A., Neff, J., Rothenberg, D., Thomas, E., Thornton, P.E., Zender, C.S., 2010. Observed 20th century desert dust variability: impact on climate and biogeochemistry. Atmos. Chem. Phys. 10, 10875–10893. https://doi.org/10.5194/acp-10-10875-2010.

Mazzei, F., D'Alessandro, A., Lucarelli, F., Nava, S., Prati, P., Valli, G., Vechi, R., 2008. Characterization of particulate matter sources in an urban environment. Sci. Total Environ. 401, 81–89. https://doi.org/10.1016/j.scitotenv.2008.03.008.

Middleton, N., 2019. Variability and trends in dust storm frequency on decadal timescales: climatic Drivers and Human Impacts. Geosciences 9 (6), 261. https://doi.org/10.3390/geosciences9060261.

Milford, C., Fernández-Camacho, R., Sánchez de la Campa, A.M., Rodríguez, R., Castell, N., Marrero, C., Bustos, J.J., de la Rosa, J., Stein, A.F., 2016. Black carbon aerosol measurements and simulation in two cities in south-west Spain. Atmos. Environ. 126, 55–65. https://doi.org/10.1016/j.atmosenv.2015.11.026.

Millán-Martínez, M., Sánchez-Rodas, D., Sánchez de la Campa, A.M., Alastuey, A., Querol, X., de la Rosa, J.D., 2021. Source contribution and origin of PM10 and arsenic in a complex industrial region (Huelva, SW Spain). Environ. Pollut. 274, 116268–116278. https://doi.org/10.1016/j.envpol.2020.116268.

Moreno, T., Querol, X., Alastuey, A., Viana, M., Salvador, P., Sánchez de la Campa, A.M., Artiñano, B., de la Rosa, J., Gibbons, W., 2006. Variations in atmospheric PM trace metal content in Spanish towns: illustrating the chemical complexity of the inorganic urban aerosol cocktail. Atmos. Environ. 40, 6791–6803. https://doi.org/10.1016/j.atmosenv.2006.05.074.

Paatero, P., 1997. Least square formulation of robuste non-negative factor analysis. Chemometr. Intell. Lab. Syst. 3, 23–35. https://doi.org/10.1016/S0169-7439(96)00044-5.

Paatero, P., Hopke, P.K., 2003. Discarding or downweighting high-noise variables in factor analytic models. Anal. Chim. Acta 490, 277–289. https://doi.org/10.1016/S0003-2670(02)01643-4.

Paatero, P., Tapper, U., 1994. Positive matrix factorization: a nonnegative factor model with optimal utilization of error estimates of data values. Environmetrics 5, 111–126. https://doi.org/10.1002/env.3170050203.

Pandolfi, M., Gonzalez-Castanedo, Y., Alastuey, A., Rosa, J.d.l., Mantilla, E., Campa, A.S. d.l., Querol, X., Pey, J., Amato, F., Moreno, T., 2011. Source apportionment of PM10 and PM2.5 at multiple sites in the strait of Gibraltar by PMF: impact of shipping emissions. Environ. Sci. Pollut. Res. 18, 260–269. https://doi.org/10.1007/s11356-010-0373-4.

Pandolfi, M., Martucci, G., Querol, X., Alastuey, A., Wilsenack, F., Frey, S., O'Dow, C.D., Dall'Osto, M., 2013. Continuous atmospheric boundary layer observations in the coastal urban area of Barcelona duringSAPUSS. Atmos. Chem. Phys. 13, 4983–4996. https://doi.org/10.5194/acp-13-4983-2013.

Pandolfi, M., Tobias, A., Alastuey, A., Sunyer, J., Schwartz, J., Lorente, J., Pey, J., Querol, X., 2014. Effect of atmospheric mixing layer depth variations on urban air quality and daily mortality during Saharan dust outbreaks. Sci. Total Environ. 494–495, 283–289. https://doi.org/10.1016/j.scitotenv.2014.07.004.

Pandolfi, M., Alastuey, A., Pérez, N., Reche, C., Castro, I., Shatalov, V., Querol, X., 2016. Trends analysis of PM source contributions and chemical tracers in NE Spain during 2004–2014: a multi-exponential approach. Atmos. Chem. Phys. 16, 11787–11805. https://doi.org/10.5194/acp-16-11787-2016.

Pérez, L., Tobias, A., Querol, X., Künzli, N., Pey, J., Alastuey, A., Viana, M., Valero, N., González-Cabré, M., Sunyer, J., 2008. Coarse particles from Saharan dust and daily mortality. Epidemiology 19 (6), 800–807. https://doi.org/10.1097/EDE.0b013e31818131cf.

Pérez, L., Tobias, A., Querol, X., Pey, J., Alastuey, A., Diaz, J., et al., 2012. Saharan dust, particulate matter and cause-specific mortality: a case-crossover study in Barcelona (Spain). Environ. Int. 48, 150–155. https://doi.org/10.1016/j.envint.2012.07.001.

Pey, J., Querol, X., Alastuey, A., Forastiere, F., Stafoggia, M., 2013. African dust outbreaks over the Mediterranean Basin during 2001–2011: PM10 concentrations, phenomenology and trends, and its relation with synoptic and mesoscale meteorology. Atmos. Chem. Phys. 13, 1395–1410. https://doi.org/10.5194/acp-13-1395-2013.

Prospero, J.M., 1999. Long-range transport of mineral dust in the global atmosphere: impact of African dust on the environment of Southeastern United States. Proc. Natl. Acad. Sci. U.S.A. 96, 3396–3403. https://doi.org/10.1073/pnas.96.7.3396.

Querol, X., Alastuey, A., de la Rosa, J.D., Sánchez dela Campa, A., Plana, F., Ruiz, C.R., 2002. Source apportionment analysis of atmospheric particulates in an industrialised urban site in southwestern Spain. Atmos. Environ. 36, 3113–3125. https://doi.org/10.1016/S1352-2310(02)00257-1.

Querol, X., Alastuey, A., Viana, M., Rodríguez, S., Artíñano, B., Salvador, P., Garcia dos Santos, S., Fernandez Patier, R., Ruiz, C.R., de la Rosa, J., Sanchez de la Campa, A. M., Menendez, M., Gil, J.I., 2004. Speciation and origin of PM10 and PM2.5 in Spain. J. Aerosol Sci. 35, 1151–1172. https://doi.org/10.1016/j.jaerosci.2004.04.002.

Querol, X., Alastuey, A., Moreno, T., Viana, M.M., Castillo, S., Pey, J., Rodríguez, S., Artiñano, B., Salvador, P., Sánchez, M., García Dos Santos, S., Herce Garraleta, M.D., Fernández-Partier, R., Moreno-Grau, S., Negral, L., Minguillón, M.C., Monfort, E., Sanz, M.J., Palomo-Marín, R., Pinilla-Gil, E., Cuevas, E., de la Rosa, J., Sánchez de la Campa, A.M., 2008. Spatial and temporal variations in airborne particulate matter (PM10 and PM2.5) across Spain 1999–2005. Atmos. Environ. 42, 3964–3979. https://doi.org/10.1016/j.atmosenv.2006.10.071.

Querol, X., Alastuey, A., Pey, J., Pandolfi, M., Cusack, M., Pérez, N., Viana, M., Moreno, T., Mihalopoulos, N., Kallos, G., Kleanthous, S., 2009. African dust contributions to mean ambient PM10 mass-levels across the Mediterranean Basin. Atmos. Environ. 43 (28), 4266–4277. https://doi.org/10.1016/j.atmosenv.2009.06.013.

Querol, X., Pérez, N., Reche, C., Ealo, M., Ripoll, A., Tur, J., Pandolfi, M., Pey, J., Salvador, P., Moreno, T., Alastuey, A., 2019. African dust and air quality over Spain: is it only dust that matters? Sci. Total Environ. 686, 737–752. https://doi.org/10.1016/j.scitotenv.2019.05.349.

Rodríguez, S., Querol, X., Alastuey, A., Kallos, G., Kakaliagou, O., 2001. Saharan dust contributions to PM10 and TSP levels in Southern and Eastern Spain. Atmos. Environ. 35, 2433–2447. https://doi.org/10.1016/S1352-2310(00)00496-9.

Rodríguez, S., Van Dingenen, R., Putaud, J.-P., Dell'Acqua, A., Pey, J., Querol, X., Alastuey, A., Chenery, S., Ho, K.-F., Harrison, R., Tardivo, R., Scarnato, B., Gemelli, V., 2007. A study on the relationship between mass concentrations, chemistry and number size distribution of urban fine aerosols in Milan, Barcelona and London. Atmos. Chem. Phys. 7, 2217–2232. https://doi.org/10.5194/acp-7-2217-2007.

Rodríguez, S., Alastuey, A., Alonso-Pérez, S., Querol, X., Cuevas, E., Abreu-Afonso, J., Viana, M., Pandolfi, M., De La Rosa, J., 2011. Transport of desert dust mixed with North African industrial pollutants in the subtropical Saharan Air Layer. Atmos. Chem. Phys. 11, 6663–6685. https://doi.org/10.5194/acp-11-6663-2011.

Sajani, S.Z., Miglio, R., Bonasoni, P., Cristofanelli, P., Marinoni, A., Sartini, C., Goldoni, C.A., Girolamo, G., Lauriola, P., 2011. Saharan dust and daily mortality in emilia–romagna (Italy) occup. Environ. Med. 68, 446–451. https://doi.org/10.1136/oem.2010.058156.

Salvador, P., Artíñano, B., Molero, F., Viana, M., Pey, J., Alastuey, A., Querol, X., 2013. African dust contribution to ambient aerosol levels across central Spain: characterization of long-range transport episodes of desert dust. Atmos. Res. 127, 117–129. https://doi.org/10.1016/j.atmosres.2011.12.011.

Salvador, P., Alonso, S., Pey, J., Artíñano, B., de Bustos, J.J., Alastuey, A., Querol, X., 2014. African dust outbreaks over the western Mediterranean basin: 11 year characterization of atmospheric circulation patterns and dust source areas. Atmos. Chem. Phys. 14, 6759–6775. https://doi.org/10.5194/acp-14-6759-2014.

Salvador, P., Molero, F., Fernandez, A.J., Tobías, A., Pandolfi, M., Gómez-Moreno, F.J., Barreiro, M., Pérez, N., Marco, I.M., Revuelta, M.A., Querol, X., Artiñano, B., 2019. Synergistic effect of the occurrence of African dust outbreaks on atmospheric pollutant levels in the Madrid metropolitan area. Atmos. Res. 226, 208–218. https://doi.org/10.1016/j.atmosres.2019.04.025.

Sánchez de la Campa, A.M., de la Rosa, J.D., 2014. Implications for air quality and the impact of financial and economic crisis in South Spain: geochemical evolution of atmospheric aerosol in the ceramic region of Bailén. Atmos. Environ. 98, 519–529. https://doi.org/10.1016/j.atmosenv.2014.09.023.

Sánchez de la Campa, A.M., de la Rosa, J., Querol, X., Alastuey, A., Mantilla, E., 2007. Geochemistry and origin of PM10 in the Huelva region, southwestern Spain. Environ. Res. 103, 305–316. https://doi.org/10.1016/j.envres.2006.06.011.

Sánchez de la Campa, A.M., de la Rosa, J.D., González-Castanedo, Y., Fernández-Camacho, R., Alastuey, A., Querol, X., Pio, C., 2010. High concentrations of heavy metals in PM from ceramic factories of Southern Spain. Atmos. Res. 96, 633–644. https://doi.org/10.1016/j.atmosres.2010.02.011.

Sánchez de la Campa, A., Moreno, T., De La Rosa, J., Alastuey, A., Querol, X., 2011. Size distribution and chemical composition of metalliferous stack emission particles in the San Roque petroleum refinery complex, southern Spain. J. Hazard Mater. 190, 713–722. https://doi.org/10.1016/j.jhazmat.2011.03.104.

Sánchez de la Campa, A.M., Sánchez-Rodas, D., Alsioufi, L., Alastuey, A., Querol, X., Jesús, D., 2018. Air quality trends in an industrialised area of SW Spain. J. Clean. Prod. 186, 465–474. https://doi.org/10.1016/j.jclepro.2018.03.122.

Sánchez-Rodas, S., Alsioufi, L., Sanchez De La Campa, A.M., Gonzalez-Castanedo, Y., 2017. Antimony speciation as geochemical tracer for anthropogenic emissions of atmospheric particulate matter. J. Hazard Mater. 324, 213–220. https://doi.org/10.1016/j.jhazmat.2016.10.051.

Stafoggia, M., Zauli-Sajani, S., Pey, J., Samoli, E., Alessandrini, E., Basagaña, X., Cernigliaro, A., Chiusolo, M., Demaria, M., Díaz, J., et al., 2016. Desert dust outbreaks in Southern Europe: contribution to daily PM10 concentrations and short-term associations with mortality and hospital admissions. Environ. Health Perspect. 124, 413–419. https://doi.org/10.1289/ehp.1409164.

Stein, A.F., Draxler, R.R., Rolph, G.D., Stunder, B.J.B., Cohen, M.D., Ngan, F., 2015. NOAA's HYSPLIT atmospheric transport and dispersion modelling system. Bull. Am. Meteorol. Soc. 96, 2059–2077. https://doi.org/10.1175/BAMS-D-14-00110.1.

Tobías, A., Pérez, L., Díaz, J., Linares, C., Pey, J., Alastruey, A., Querol, X., 2011. Short-term effects of particulate matter on total mortality during Saharan dust outbreaks: a case–crossover analysis in Madrid (Spain). Sci. Total Environ. 412–413, 386–389. https://doi.org/10.1016/j.scitotenv.2011.10.027.

Tobías, A., Rivas, I., Reche, C., Alastuey, A., Rodríguez, S., Fernández-Camacho, R., Querol, X., 2018. Short-term effects of ultrafine particles on daily mortality by primary vehicle exhaust versus secondary origin in three Spanish cities. Environ. Int. 111, 144–151. https://doi.org/10.1016/j.envint.2017.11.015.

Twohy, C.H., Kreidenweis, S.M., Eidhammer, T., Browell, E.V., Heymsfield, A.J., Bansemer, A.R., Anderson, B.E., Chen, G., Ismail, S., DeMott, P.J., Van Den Heever, S.C., 2009. Saharan dust particles nucleate droplets in eastern Atlantic clouds. Geophys. Res. Lett. 36, L01807. https://doi:10.1029/2008GL035846.

UNE-EN 12341, 2015. Standard Gravimetric Measurement Method for Determination of the PM10 or PM2.5 Mass Concentration of Suspended Particulate Matter.

Viana, M., Querol, X., Alastuey, A., Cuevas, E., Rodríguez, S., 2002. Influence of African dust on the levels of atmospheric particulates in the Canary Islands air quality network. Atmos. Environ. 36, 5751–5875. https://doi.org/10.1016/S1352-2310(02)00463-6.

Zhang, X., Zhao, L., Tong, D., Wu, G., Dan, M., Teng, B.A., 2016. Systematic review of global desert dust and associated human health effects. Atmosphere 7, 158. https://doi.org/10.3390/atmos7120158.

Chemosphere 303 (2022) 134853

Contents lists available at ScienceDirect

Chemosphere

journal homepage: www.elsevier.com/locate/chemosphere

Impact of the SARS-CoV-2 lockdown measures in Southern Spain on PM10 trace element and gaseous pollutant concentrations

María Millán-Martínez [a,b,*], Daniel Sánchez-Rodas [a,b], Ana M. Sánchez de la Campa [a,c], Jesús de la Rosa [a,c]

[a] Associate Unit CSIC-University of Huelva "Atmospheric Pollution", Center for Research in Sustainable Chemistry - CIQSO, University of Huelva, E21071, Huelva, Spain
[b] Department of Chemistry, Faculty of Experimental Sciences, University of Huelva, Campus El Carmen s/n, 21071, Huelva, Spain
[c] Department of Earth Science, Faculty of Experimental Sciences, University of Huelva, Campus El Carmen s/n, 21071, Huelva, Spain

HIGHLIGHTS

- The effect of Covid-19 lockdown over air pollutants has been studied at Andalusia.
- PM10 trace elements and NO_2 levels, related to traffic, were highly reduced.
- General conclusions for industrial sites cannot be drawn.

GRAPHICAL ABSTRACT

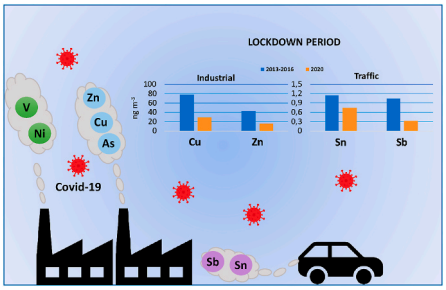

ARTICLE INFO

Handling Editor: Dr. R Ebinghaus

Keywords:
Lockdown
Covid-19
PM10 trace elements
Industrial activity
Traffic

ABSTRACT

Trace element concentrations within PM10, gaseous pollutants (NO_2 and SO_2), and PM10 levels were studied during the Covid-19 lockdown at a regional level in Southern Spain (Andalusia). Pollutant concentrations were compared considering different mobility periods (pre-lockdown, lockdown, and relaxation) in 2020 and previous years (2013–2016). An acute decrease in NO_2 levels (<50%) was observed as a consequence of traffic diminution during the confinement period. Moreover, a lower reduction in PM10 levels and a non-clear pattern for SO_2 levels were observed.

During the lockdown period, PM10 elements released from traffic emissions (Sn and Sb) showed the highest concentration diminution in the study area. Regarding the primary industrial sites, there were no significant differences in V, Ni, La, and Cr concentration reduction during 2020 associated with industrial activity (stainless steel and oil refinery) in Algeciras Bay. Similarly, concentrations of Zn showed the same behaviour at Cordoba, indicating that the Zn-smelter activity was not affected by the lockdown. Nevertheless, stronger reductions of Cu, Zn, and As in Huelva during the confinement period indicated a decrease in the nearby Cu-smelter emissions. Brick factories in Bailen were also influenced by the confinement measures, as corroborated by the marked decrease in concentrations of Ni, V, Cu, and Zn during the lockdown compared to that from previous years.

* Corresponding author. Associate Unit CSIC-University of Huelva "Atmospheric Pollution", Center for Research in Sustainable Chemistry - CIQSO, University of Huelva, E21071, Huelva, Spain.
E-mail address: maria.millan@dqcm.uhu.es (M. Millán-Martínez).

https://doi.org/10.1016/j.chemosphere.2022.134853
Received 10 February 2022; Received in revised form 23 April 2022; Accepted 3 May 2022
Available online 7 May 2022

This work has shown the baseline concentrations of trace elements of PM10, which is of great value to air quality managers in order to minimise pollution levels by applying the confinement of the population, affecting both traffic and industrial anthropogenic activities.

1. Introduction

By the end of 2019, the first case of Covid-19 (derived from the coronavirus SARS-CoV-2) was reported in Wuhan (China). The virus rapidly spread into Europe throughout Italy, and on 11th March a global pandemic was declared by the World Health Organization (WHO, 2020a). Since then, several countries have established lockdown measures to minimise the number of people infected. With the aim of diminishing human mobility, most economic activities, except those for essential purposes, were reduced. Consequently, flights, trains, and vehicular and public transportation were stopped. This exceptional situation supposed an enormous change from a social, economic, and environmental point of view.

The scientific community took this opportunity to study air quality with less human influence on the environment. TROPOMI and OMI satellite image analysis showed that NO_2 levels decreased in China (40%), South Korea (30%), the United States (42–48%), and Western Europe (20–38%) (Bauwens et al., 2020) during the corresponding confinement periods. Other studies in China have also reported the reduction of gaseous pollutants and PM10 and PM2.5, as a result of lower emissions from road traffic and coal combustion (Xu et al., 2020; Silver et al., 2020). Furthermore, a marked decrease in PM2.5 concentrations was observed in India and the USA, especially in major urban cities with traffic influence (Chen et al., 2020; Mahato and Ghosh, 2020). However, these observations did not always apply to SO_2 levels, which experienced only a slight decrease (Shi and Brasseur, 2020; Kandari and Kumar, 2021). SO_2 emissions were associated with coal burning for residential heating and energy production, and these activities were not suspended during the confinement periods. Apart from evaluating the drop in air pollutant concentrations, other studies have emphasised the relationship between exposure to atmospheric pollution and Covid-19 deaths (Wu et al., 2020; Shakoor et al., 2020). It has been demonstrated that the presence of certain air pollutants (i.e. NO_2, PM10, and PM2.5) increases respiratory and cardiovascular health problems. Therefore, polluted air can involve an extra risk, considering that the virus spreads by droplet and aerosol transmission (Wang and Du, 2020; Zhu et al., 2020; Naqvi et al., 2021).

The Covid-19 virus quickly reached Europe at the end of March 2020; therefore, restriction measures were taken across the territory. Filonchyk et al. (2021) showed the greatest reduction in PM10 and PM2.5 concentrations in April and March 2020 compared to the same period in 2019 in large cities of Poland. Other European cities from the UK and Italy found a clear decrease in NO_x levels, while SO_2 did not have the same pattern at all monitoring sites (Collivignarelli et al., 2020; Donzelli et al., 2020; Higham et al., 2021; Wyche et al., 2021). In spite of the numerous works mentioned above, all of them focus on the study of gaseous and particulate matter (PM) concentration changes, neglecting its chemical composition.

Spain is one of the countries most affected by Covid-19, becoming the fifth state with the highest number of cases (WHO, 2020b). On 14th March, Spain's President declared a state of emergency, imposing a lockdown across the country and limiting all unnecessary displacements of the people. The confinement period in Spain was approximately two months followed by a progressive relaxation period. Subsequently, a "new normal" was created. In addition to the rest of the world, many research groups have studied the changes in air quality in Spain considering these three periods. The authors concluded in an important reduction in NO_x, NO_2, and NO emissions (~40–60%) due to the diminution of road traffic, notably in large cities such as Madrid, Barcelona, and Valencia (Baldasano, 2020; Tobías et al., 2020; Donzelli et al., 2021). The PM concentrations also decreased in these cities (30% PM10), although variations in PM2.5 values were less pronounced because this secondary pollutant has other potential emission sources such as industry, farming, or agricultural biomass burning, but also because of the contribution of secondary component to its total mass concentration. Another important finding was the relative change in SO_2 and CO levels: a smaller decrease or increase was observed because of their origin from specific industrial activities, cargo shipping, or domestic coal heating, which were less affected by government restrictions (Martorell-Marugán et al., 2021; Querol et al., 2021). All of the above works concurred that the confinement imposed in 2020 has offered to the scientific community ideal conditions to study the factors most implied in air quality improvement. Nevertheless, there is no background information about the influence of mobility measures on the PM chemical composition. Until now, most of the authors have focused on gaseous pollutants and changes in PM10 levels. They coincided with a lower decrease in PM10 concentrations compared to NO_2 levels. In this sense, it is interesting to emphasise the complex origin of PM given the physicochemical variety of its components and sources (Moreno et al., 2006). Thus, understanding the evolution of the PM chemical composition during the lockdown should allow a better comprehension of the PM diminution origin and its respective sources.

In this study, we aimed to assess the change in PM10 trace elements during the year 2020 at a regional level (Andalusia, Southern Spain) as a consequence of the adopted lockdown to avoid the spread of Covid-19. For this purpose, the concentrations of PM10 trace elements related to traffic and industrial emissions obtained during 2020 were compared to values recorded in earlier periods (2013–2016). Furthermore, we provide gaseous pollutants (SO_2 and NO_2) and PM10 levels during this year with mobility restrictions. These results can be used in the future to improve air quality in areas with a significant contribution of traffic and industry.

2. Methodology

2.1. Study area

Andalusia is the southernmost region of the Iberian Peninsula and the largest community in Spain (approximately 8.5 million inhabitants, INE, 2021). This region is separated from North Africa by the Strait of Gibraltar, where the Mediterranean Sea (East) and the Atlantic Ocean (West) meet (Fig. 1). The topography of Andalusia encompasses three different areas: the Sierra Morena Range in the north, the Baetic Mountains in the south, and the basin of the Guadalquivir River lies between these two mountainous areas. The climate in Andalusia is generally Mediterranean (hot summers and mild winters), with great variation due to its complex topography: the weather is dryer in the east, and rainfall increases in the coastal locations. Furthermore, a more continental climate is found in areas adjacent to the main mountainous ranges. North African dust outbreaks affect the air quality of Andalusia, which normally occurs during February, March, and summer months. (Rodríguez et al., 2001; Cachorro et al., 2008; Fernández-Camacho et al., 2010; Millán-Martínez et al., 2021b).

The economy of Andalusia is primarily based on service and agricultural sectors, although there are also important industrial estates located across the territory. In this sense, several studies highlight emissions related to different industrial activities. High concentrations of SO_2, and certain toxic metals released from metallurgic processes, ceramic industries, and oil refineries are some examples (Querol et al., 2004, 2008; de la Rosa et al., 2010; Pandolfi et al., 2011; Sánchez de la

Campa et al., 2018; Millán-Martínez et al., 2021a, 2021b). Another important source of pollution in Andalusia is road traffic. The levels of NO_2 and PM10 are higher in populated urban areas because public transportation is, in most cases, insufficient (de la Rosa et al., 2010; Amato et al., 2014).

For PM10 geochemical composition characterisation purposes, 12 monitoring sites belonging to the Air Quality Monitoring Network of the Regional Government of Andalusia were considered in this study. They are distributed in the eight provinces of Andalusia (Fig. 1) and were selected considering their environments and nearby emission sources.

1. Four traffic monitoring stations: Principes (Seville), Palacio Congresos (Granada), Carranque (Malaga), and Mediterraneo (Almeria). These sites are located in metropolitan areas of some of the most populated cities of Andalusia (Seville, 700,000 inhabitants; Malaga 578,000 inhabitants, INE, 2021) and, hence, are affected by dense urban traffic emissions. The air quality in these locations has been previously studied (Fernández-Camacho et al., 2016; Sánchez-Rodas et al., 2017).
2. Five urban-industrial monitoring stations: Campus (Huelva), La Rabida (Huelva), Nerva (Huelva), Puente Mayorga (Cadiz), and Bailen (Jaen). Campus and La Rabida sites have been broadly studied because of the industrial estates established in this area. Thus, the emission of sulphide-related trace elements in PM10 (As, Se, Cd, Sb, Bi, or Pb) from a Cu-smelter has been the principal geochemical anomaly found in many studies (Chen et al., 2016; Sánchez de la Campa et al., 2018; Millán-Martínez et al., 2021a). The Nerva monitoring station is located in the vicinity of a mining district (Riotinto) characterised by sulphide geochemical anomalies derived from fugitive emissions (Sánchez de la Campa et al., 2020). Very close to the Strait of Gibraltar (Algeciras Bay, Cadiz) (Fig. 1) are located a petrochemical plant and oil refinery, a power plant, and a stainless-steel industry. Considering this industrial activity and the high maritime transport, high concentrations of Cr, V, and Ni have been reported in the nearby selected monitoring sites (La Linea, Fig. 1) (de la Rosa et al., 2010; Pandolfi et al., 2011). Bailen is another industrial site characterised by the presence of one of the largest ceramic industries in Spain (Sánchez de la Campa et al., 2010; Sánchez de la Campa and de la Rosa, 2014).
3. Two urban monitoring stations, San Fernando (Cadiz) and Lepanto (Cordoba). The latter is affected by emissions from not-too-far metallurgy factories (Sánchez-Rodas et al., 2017).
4. One rural monitoring station was Matalascañas (Huelva). This monitoring site is situated on the eastern coastline of Huelva, 30 km from the industrial estate already mentioned for the Campus site. Furthermore, Matalascañas is within Doñana National Park, declared a UNESCO "World Reserve of the Biosphere".

To evaluate the Covid-19 restriction measures over the concentration of pollutants, we compared the following subperiods:

1. The pre-lockdown period: 1st February to 15th March when the state of emergency was declared in Spain.
2. Lockdown period: 16th March to 10th May when a relaxation period was established.
3. Relaxation period: 11th May to 31st July. In Spain, different relaxation measures were taken depending on the region (Querol et al., 2021), but in Andalusia, this relaxation applied to nearly the entire territory.

These three sub-periods were studied for PM10 trace element concentrations comparing the year 2020 to the average concentrations obtained during 2013–2016, since no data were available during 2017–2019.

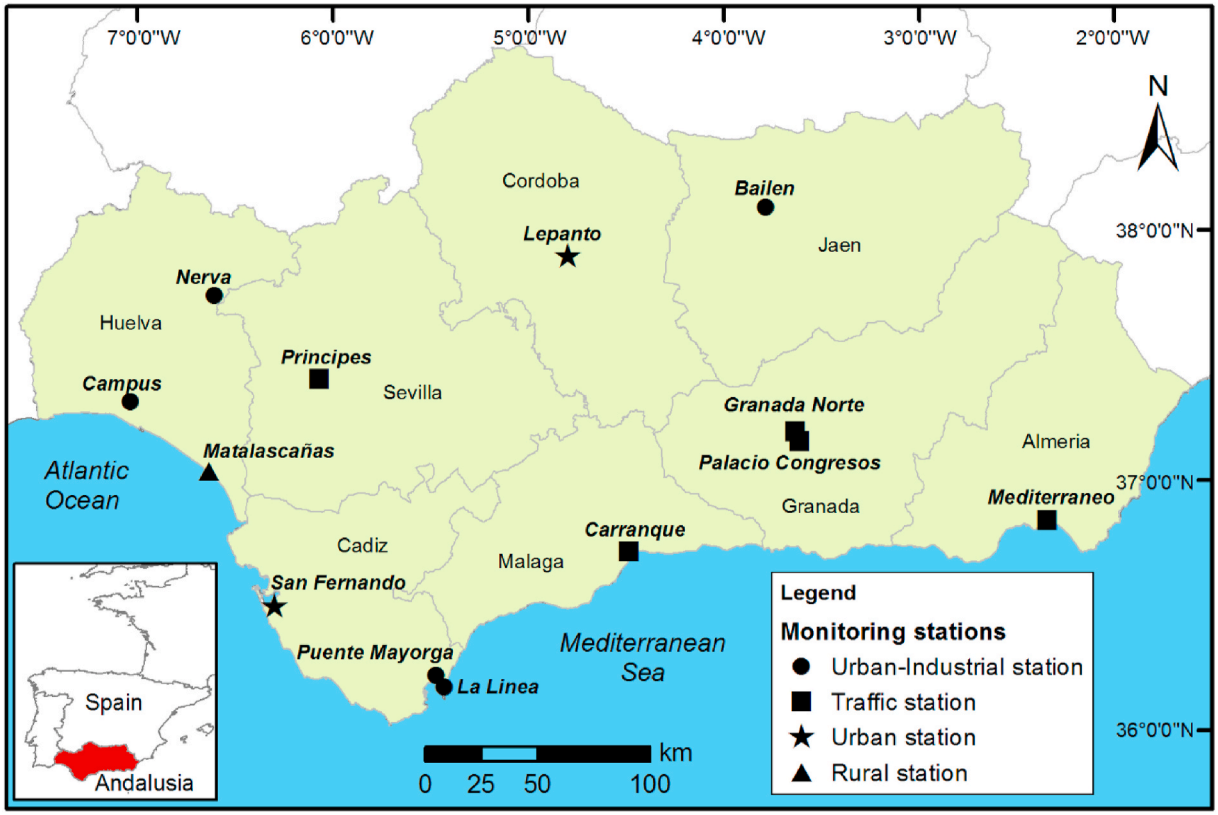

Fig. 1. Map of the study area indicating the provinces and the monitoring stations.

2.2. Industrial activity

The confinement imposed in 2020 supposed strict mobility restrictions and, thus, a direct impact on transport and traffic-related atmospheric emissions. Nevertheless, essential services were not wholly suppressed; therefore, the influence of the lockdown on the industrial sector remains unclear. It has already been mentioned that some monitoring stations are influenced by different industrial activity emissions in Andalusia. Consequently, it is very important to study the main air pollutant emissions derived from these activities during 2020 and previous years using the European Pollutant Emission Register (EPER, 2021). Furthermore, Emissions Inventory of Andalusia Government (2003–2019) has been consulted in order to select the main pollutant contributions in the different Andalusian provinces (https://bit.ly/38QfZxE). From this inventory, it can be inferred that the most representative emissions correspond to several activities located at specific industrial estates (Huelva, Algeciras Bay and Bailen).

In the province of Huelva, several industrial estates affect the monitoring sites of Campus and La Rabida (Millan-Martínez et al., 2021a). The predominant activities contributing to SO_2 emissions are an oil refinery (La Rabida) and a Cu-smelter, and to a much lesser extent, the TiO_2 pigment manufacturing industry. Comparing SO_2 emissions to those obtained in previous years (Fig. S1), a no relevant variation can be observed in 2020. The production of Cu is also responsible for the release of Cu and other sulphide-related elements such as Zn, As, Sb, and Pb, which have significantly decreased over the years (Fig. S1). Attending to Ni emissions coming from the refinery, a decreasing trend was noticed beginning in 2015, whereas Ni levels from the Cu-smelter were higher in 2020 than in previous years.

The other relevant industrial area of Andalusia corresponds to the Algeciras Bay (province of Cadiz, Fig. 1), where is located the Puente Mayorga monitoring station. In this case, SO_2 levels proceed from an oil refinery and a coal-fired power station, which has been inactive since March 2019. Furthermore, the substitution of coke as fuel by natural gas in the oil refinery has resulted in a progressive decrease in SO_2 emissions since 2015 (Fig. S2). High Cr emissions have also been registered in the area, primarily as a result of the presence of a stainless-steel manufacturing plant (Pandolfi et al., 2011; Millán-Martínez et al., 2021b). The amount of Cr emitted from this industry does not present a high variation in 2020 (Fig. S2), but considering the oil refinery, the emissions of Cr have decreased significantly since 2014.

Finally, the ceramic industry (brick and pottery) is highly developed in the city of Bailen (province of Jaen, Fig. 1). These activities are characterised by the emissions of air pollutants such as SO_2, Ni, Zn, Pb, and Cu derived from coke combustion emission plumes (Sánchez de la Campa et al., 2010). Selecting a representative ceramic industry, a reduction in the emissions of these pollutants has been observed in 2020 (Fig. S3).

2.3. PM sampling and analysis

During 2020, PM10 sampling was performed using low-volume captors (DIGITEL DPA14; 58 m^3 day^{-1}). Sampling frequency was one filter every six days for a duration of 24 h. Furthermore, intensive campaigns were also performed at the industrial monitoring stations of Puente Mayorga and Campus (192 and 184 filters/year, respectively). Quartz glass filters were used to collect PM10.

For PM10 chemical analysis, a half fraction of each filter was acid digested (2.5 mL HNO_3: 5 mL HF: 2.5 mL $HClO_4$) for the analysis of trace elements by ICP-MS (Agilent model, 7900) using a modified method proposed by Querol et al. (2001). For quality control, analysis of the NIST-1633c (fly ash, Standard Reference Material) was carried out during every analytical run of the ICP-MS methodology. The digestion procedure of the PM10 samples and ICP-MS analysis were also validated using NIST-1648a (urban particulate matter, Standard Reference Material). External calibration was performed by ICP-MS using 1, 2, and 4 Agilent® multielemental solutions (1–250 μg L^{-1}, as well as HNO_3 5% blank). To minimise the possible fluctuations in the plasma, ^{103}Rh was used as an internal standard. The average precision and accuracy fall for most of the elements under typical analytical errors (in the range of 5–10%).

PM10 chemical information obtained in 2020 was compared to the mean values from 2013 to 2016. In addition, PM10 and gaseous pollutant levels (NO_2 and SO_2), recorded by the corresponding automatic instrumentation (reference methods, EU 2008), were studied during 2020 and the period 2013–2016. In this respect, the monitoring stations Granada Norte site, next to Palacio Congresos, and La Linea site in Algeciras Bay (Fig. 1), were also considered.

3. Results and discussion

3.1. Pluviometry and air masses origin

It is widely known that dust coming from the Saharan desert is often transported to Southern Europe, causing an increase in PM10 levels (Viana et al., 2002; Querol et al., 2009; Salvador et al., 2013). For this reason, it is important to consider these events during the study period. To this end, air masses in the monitoring stations were studied considering two representative locations: Western Andalusia (37° N, 6° W) and Eastern Andalusia (37° N, 3° W). A five-day back-trajectory analysis starting at three different altitudes (500, 1500, and 2500 m a. s.l.) was carried out using the HYSPLIT model (Stein et al., 2015) of the NOAA Air Resources Laboratory (ARL) (https://www.ready.noaa.gov/HYSPLIT.php). Additionally, North African dust events affecting the monitoring stations were also studied using aerosol, dust maps, and satellite images from NRL (http://www.nrlmry.navy.mil/aerosol), SKIRON (https://forecast.uoa.gr/en/forecast-maps/dust/north-atlantic), BSC DUST (https://ess.bsc.es/bsc-dust-daily-forecast), and Earth Data NASA project (https://worldview.earthdata.nasa.gov/).

The daily atmospheric episodes are classified as North African (NAF) when an African dust outbreak occurs, Atlantic (ATL), including the ones from N, NW, SW, and W Atlantic air masses, and other minor air mass origins (regional, Mediterranean, and European origins >5%).

By analysing the mass origin frequency during 2020 and the period 2013–2016, we found Atlantic to be the most frequent origin for Western (58% and 62%, respectively) and Eastern Andalusia (46% and 52%, respectively). In addition, when comparing air masses during lockdown months, similar NAF events occurred for 2013–2016 and 2020: 30% and 34% for Western Andalusia, and 41% and 44% for Eastern Andalusia (Fig. S4).

Rainfall is another relevant driving parameter for pollutant levels since it is well known that precipitation can “wash” the atmosphere and result in the deposition of air pollutants. Data from the Spanish State Meteorological Agency show that during lockdown months in 2020, cumulative precipitation was 80 L, which is comparable to the average obtained for the period 2013–2016 (74 L) for the same months.

3.2. Gaseous pollutants and PM10 levels

The percentages of change in NO_2, SO_2, and PM10 levels in 2020 are shown in Table 1 for each monitoring site compared to the same subperiods in 2013–2016. A general overview reveals an important decrease in NO_2 emissions and PM10 levels in most of the monitoring sites during confinement. In the case of SO_2, a clear pattern is not observed.

During the lockdown period, NO_2 levels were reduced by half in most of the monitoring sites. This fact is especially important in traffic monitoring stations with high NO_2 levels (i.e. the annual mean in Granada Norte in 2016 was 44 μg NO_2 m^{-3}), where the annual NO_2 concentration standard (40 μg m^{-3}) established by European directives (EU, 2008) is sometimes exceeded. The primary NO_2 anthropogenic sources are vehicles exhaust emissions and fossil fuel combustion

Table 1
Variation of percentages in 2020 pollutants levels at the considered monitoring stations of Andalusia during the pre-lockdown, lockdown and relaxation periods, compared with the respective averaged values for the same three periods in 2013–2016.

MONITORING STATION		PRE-LOCKDOWN	LOCKDOWN	RELAXATION
TRAFFIC				
Granada Norte	SO_2	−30	−20	−9
	NO_2	8	−58	−20
	PM10	11	−35	−11
Principes	SO_2	−17	−31	−22
	NO_2	−21	−61	−41
	PM10	8	−33	−15
Carranque	SO_2	−76	−79	−53
	NO_2	7	−55	−11
	PM10	7	−23	−23
Mediterraneo	SO_2	−55	−64	−72
	NO_2	−6	−66	−29
	PM10	20	−41	−28
URBAN-INDUSTRIAL				
Bailen	SO_2	25	−2	20
	NO_2	−1	−55	−2
	PM10	−4	−41	−12
Campus	SO_2	80	−1	−5
	NO_2	35	−35	−36
	PM10	1	−12	−5
La Linea	SO_2	−77	−84	−82
	NO_2	−19	−58	−37
	PM10	−26	−34	−37
URBAN				
Lepanto	SO_2	−34	−47	−20
	NO_2	−11	−72	−40
	PM10	30	−27	−4
San Fernando	SO_2	−67	−76	−62
	NO_2	−26	−77	−25
	PM10	11	−13	7
RURAL				
Matalascañas	SO_2	−13	33	39
	NO_2	−18		−71
	PM10	15	3	−19

(Hesterberg et al., 2009), and in Spain, more than 75% of NO_2 emissions are due to road traffic (MITECO, 2020). This gaseous pollutant contributes to the formation of PM2.5, and O_3 in the air, representing a human health risk (Santurtún et al., 2017). Fig. 2 shows a pronounced decrease in NO_2 levels corresponding to the beginning of the lockdown period at the traffic monitoring stations. Although levels tended to recover during the relaxation period, they did not reach the values recorded in January 2020. This is due to the mobility restrictions imposed by the Spanish government between certain regions, as well as the enhancement of teleworking with the aim of avoiding human contact. Therefore, the influence of the lockdown on traffic emissions and the corresponding NO_2 level reduction in Andalusia agrees with previously published results in other regions of Spain (Baldasano, 2020; Tobías et al., 2020; Querol et al., 2021; Ceballos-Santos et al., 2021; Donzelli et al., 2021).

In the case of PM10 levels, a less marked decrease occurred in the study area. PM10 concentrations were reduced between 12% and 41%, with the highest variation in the inland cities of Andalusia. There are various sources that contribute to the total mass content of PM10; marine aerosols and mineral dust from natural resuspension are two of the primary sources. This could explain why Campus (urban-industrial) and Matalascañas (rural) PM10 levels remained stable or slightly decreased during the lockdown period. These monitoring stations, located in the western part of Andalusia, have a high contribution of mineral dust and marine aerosols to PM10 (Millán-Martínez et al., 2021) and are strongly affected by NAF episodes. Nevertheless, a PM10 chemical composition study is needed to comprehend the actual origin of the decrease.

SO_2 is a gaseous pollutant generated by high-temperature processes such as industrial activities, energy production or domestic heating. In Andalusia, 34% of SO_2 emissions were derived from oil refineries (EPER, 2019). SO_2 levels are normally low, not higher than 10 μg m^{-3}, and small differences in concentrations could involve high variation percentages. The European normative does not establish any annual SO_2 limit; however, it is recommended that it does not exceed 350 SO_2 $\mu g \cdot m^{-3} \cdot h^{-1}$ more than 24 times per year. This target value is rarely exceeded; nevertheless, sporadic hourly SO_2 peaks (>20 μg m^{-3} h^{-1}) have often been measured at industrial sites. In this sense, it is more interesting to evaluate the number of days with SO_2 impacts over the previous years to those in 2020.

The monitoring stations of Campus and Puente Mayorga have been previously described because of the high industrial influence of the oil refineries, petrochemical plants, and metallurgic activities developed in the area (Pandolfi et al., 2011; Sánchez de la Campa et al., 2018). In Fig. 3, it can be clearly seen that there has been no decrease in SO_2 impact days in Campus since 2012. In the case of Puente Mayorga, impact days started to be reduced from 2018 to 2020, possibly as a result of the use of natural gas as fuel in several industrial activities (personal communication). This is in concordance with the high reduction percentage of SO_2 levels in La Linea, not only in the lockdown period.

Analysing the year 2020, impact days became lower than in Campus over several months, contrary to what has been observed in previous

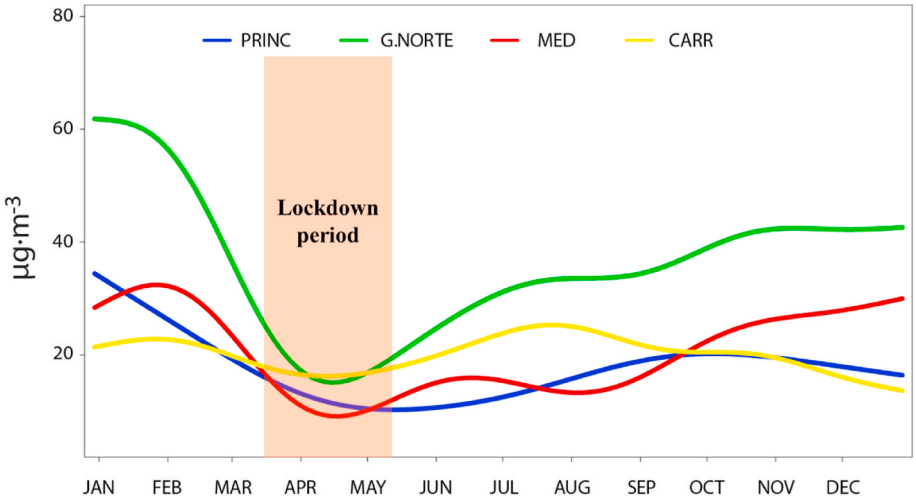

Fig. 2. Time variation of NO_2 concentrations during the year 2020 at the traffic monitoring stations considered in this study. PRINC: Principes; G.NORTE: Granada Norte; MED: Mediterraneo; CARR: Carranque.

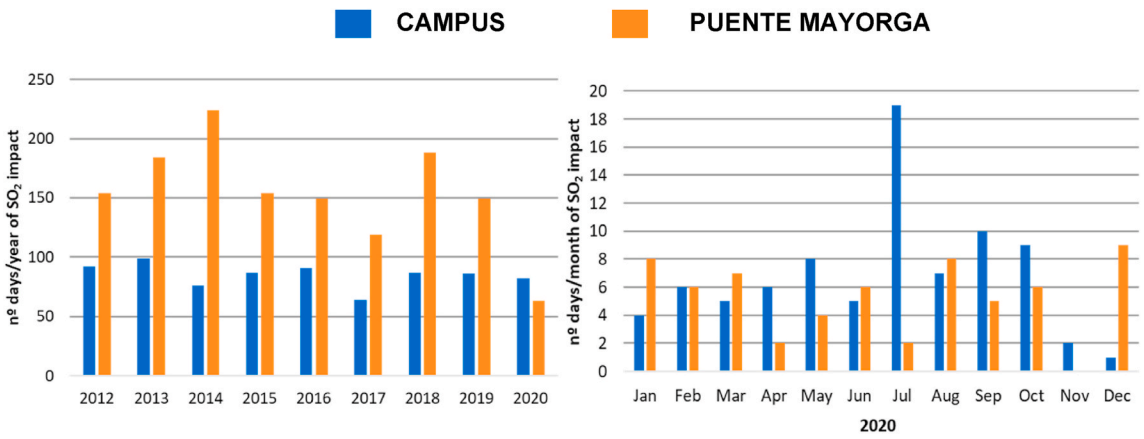

Fig. 3. SO_2 impacts days per year in the period 2012–2020 (left) and per month during 2020 at the urban-industrial monitoring stations of Campus and Puente Mayorga.

years. Another important observation is the slight reduction of the SO_2 impact days in March in Campus, whereas in Puente Mayorga, impacts are higher in March than in February. Nevertheless, SO_2 concentrations are highly dependent on the wind regimes, making it more difficult to evaluate industrial activity during the lockdown period.

In summary, as a consequence of the Covid-19 adopted measures, there was a remarkable reduction in NO_2 emissions at a regional level as a result of the lower traffic during the stay-home period. To a lesser extent, due to the contribution of natural sources, lockdown measures also resulted in a decreasing pattern in PM10 levels in most cases. A different scenario was observed for SO_2 levels, with no clear trends in change percentage and impact days during the lockdown period.

3.3. Geochemical maps of PM10 trace elements (2020 vs 2013–2016)

Annual average concentrations of main PM10 trace elements during 2020 are summarized in Table 2 and represented in more detail in the geochemical maps in Fig. S5. When comparing with the mean concentrations obtained for the period 2013–2016 certain anomalies are still observed in 2020 as a consequence of traffic or specific industrial emissions.

V and Ni are two elements whose emissions are derived from industrial activities such as oil refineries, coal-fired power plants, and maritime transport from fuel-oil combustion. Previous studies have highlighted the high Ni and V concentrations in PM10 in Puente Mayorga as a consequence of industrial estate emissions (Moreno et al.,

Table 2
Mean PM10 trace elements concentrations (in ng m^{-3}) at the monitoring stations of Andalusia during 2020. P.CON: Palacio Congresos; PRINC: Principes; MED: Mediterraneo; CARR: Carranque; PMAY: Puente Mayorga; CAMP: Campus; BAIL: Bailen; RAB: La Rabida; NERV: Nerva; LEP: Lepanto; S.FER: San Fernando; MAT: Matalascañas.

Monitoring station	Traffic				Urban-Industrial					Urban		Rural
	P·CON	PRINC	MED	CARR	PMAY	CAMP	BAIL	RAB	NERV	LEP	S.FER	MAT
N, ng m^{-3}	54	61	60	59	192	184	64	58	63	62	59	62
Li	0.78	0.41	0.39	0.26	0.23	0.29	0.68	0.33	0.59	0.48	0.23	0.31
Be	0.02	0.02	0.01	0.01	0.01	0.01	0.03	0.01	0.02	0.03	0.01	0.06
Sc	0.17	0.12	0.10	0.08	0.05	0.09	0.15	0.10	0.18	0.13	0.07	0.08
V	3.28	1.79	2.75	4.08	2.55	1.60	23.71	1.91	1.71	1.76	1.65	1.39
Cr	3.46	3.34	3.21	2.94	13.1	1.24	2.32	2.36	1.57	2.56	1.75	1.12
Co	0.25	0.20	0.18	0.16	0.33	0.14	0.24	0.28	0.28	0.17	0.10	0.13
Ni	2.98	3.45	3.10	3.14	6.59	1.32	6.90	2.54	1.45	1.62	2.41	1.38
Cu	8.88	13.5	7.74	9.26	7.48	21.2	5.95	276	12.8	20.3	3.30	30.4
Zn	21.5	34.3	16.2	26.1	39.7	16.8	24.2	60.4	14.5	80.7	14.1	19.1
Ga	0.30	0.20	0.15	0.14	0.11	0.13	0.29	0.15	0.27	0.26	0.11	0.11
Ge	0.33	0.31	0.39	0.31	0.12	0.13	0.32	0.16	0.14	0.42	0.33	0.11
As	0.41	0.87	0.51	0.33	0.36	3.29	0.46	6.11	1.61	0.51	0.41	0.94
Se	0.10	0.12	0.10	0.10	0.04	0.12	0.13	0.19	0.13	0.14	0.13	0.10
Rb	1.50	0.98	0.67	0.71	0.32	0.68	2.14	0.76	1.18	1.87	0.47	0.60
Sr	11.0	3.97	4.83	3.24	2.28	2.07	5.33	3.59	3.37	4.19	3.40	3.32
Y	0.69	0.68	0.47	0.55	0.17	0.27	0.62	0.33	0.41	0.67	0.51	0.26
Zr	3.23	3.45	3.36	3.05	0.73	2.46	3.27	1.60	3.11	3.38	2.60	1.44
Mo	11.6	11.7	8.28	11.1	0.60	2.41	9.36	5.01	4.44	8.19	10.5	3.63
Cd	0.07	0.08	0.06	0.07	0.29	0.37	0.08	0.61	0.11	0.30	0.03	0.10
Sn	2.06	2.46	2.14	2.44	1.39	1.28	0.88	0.97	0.65	2.24	0.84	0.60
Sb	1.26	1.58	1.02	1.16	0.55	0.66	0.79	1.23	0.48	1.24	0.33	0.24
Cs	0.07	0.04	0.04	0.02	0.02	0.03	0.11	0.03	0.06	0.10	0.02	0.02
Ba	17.9	19.2	16.2	20.9	3.12	6.92	19.2	8.73	8.77	20.9	13.8	7.11
La	0.63	0.48	0.37	0.32	1.66	0.33	0.56	0.35	0.50	0.67	0.30	0.28
W	0.03	0.03	0.03	0.03	0.08	0.02	0.04	0.08	0.10	0.08	0.03	0.09
Tl	0.01	0.01	0.03	0.01	0.01	0.02	0.25	0.03	0.02	0.07	0.00	0.01
Pb	5.28	4.98	4.06	3.19	6.05	10.8	14.5	26.6	6.37	7.32	3.32	3.63
Bi	0.12	0.34	0.18	0.17	0.12	0.57	0.15	0.85	0.26	0.21	0.16	0.10
U	0.18	0.21	0.15	0.17	0.03	0.07	0.17	0.11	0.09	0.18	0.15	0.06

2008; Pandolfi et al., 2011; Sánchez de la Campa and de la Rosa, 2014). Even though a high concentration of V was still found in Bailen in 2020 (24 ng m^{-3}), the recent use of natural gas as fuel in the nearby industries of Puente Mayorga station (CEPSA, 2020) and the inactivity of the coal-fired power plant (European Policies to reduce CO_2 emissions), resulted in a strong reduction of V concentrations (2.6 ng m^{-3} 2020 vs 22 ng m^{-3} 2013–2016). A similar situation was observed for Ni concentrations, with maximum values in Bailen (6.9 ng m^{-3}) and an important diminution in Puente Mayorga (average concentrations of 6.6 and 17 ng m^{-3} in 2020 and 2013–2016, respectively). The highest concentrations of Cr in 2020 (13 ng m^{-3}) corresponded to Puente Mayorga, derived from a stainless-steel factory located in Algeciras Bay. In addition, the catalysts used in oil refining processes can release La, explaining why this metal has the highest values in Puente Mayorga (1.7 ng m^{-3} 2020).

The concentrations of As were highest in the monitoring stations of Campus and La Rabida in 2020 (3.3 and 6.1 ng m^{-3}, respectively) due to Cu-smelter emissions in the area. As a result of this industrial activity, high concentrations of Cu, Zn, and Pb were also found in La Rabida (276, 60, and 27 ng m^{-3}, respectively in 2020). In the city of Cordoba (Lepanto monitoring station), previous studies have described high Cu and Zn concentrations from the nearest Zn-smelters (de la Rosa et al., 2010; Sánchez-Rodas et al., 2017; Millán-Martínez et al., 2021b). However, an important decrease was observed in 2020 (Cu: 20 ng m^{-3}; Zn: 81 ng m^{-3}).

Sn and Sb are typical elements released from non-exhaust traffic emissions (brake wear) (Amato et al., 2014). The brake-pads of vehicles contain Sb_2S_3 as lubricant for friction material, which is emitted as particles during break wear. The heat generated during this process can oxide considerably Sb_2S_3 (von Uexküll et al., 2005; Lijima et al., 2007; Amato et al., 2009). The related-origin of Sb with traffic emissions have been previously observed in other traffic monitoring stations of Andalusia (Sánchez-Rodas et al., 2017). Accordingly, the highest concentrations of these elements were registered in 2020 in the four traffic-monitoring stations selected for this study (Fig. S4).

In summary, the principal geochemical anomalies already described in previous years were also observed in 2020. However, the decrease or inactivity of certain industrial activities, as well as the implementation of abatement measures, have resulted in mean concentration diminutions for some trace elements. Relevant reduction percentages were registered in Puente Mayorga in V (88%) and Ni (60%) in 2020 with respect to 2013–2016. Similarly, the mean concentrations of Cu and Zn also decreased in 2020 at Campus (71% and 53%, respectively) and La Rabida (32% and 58%, respectively). In addition, the concentrations of these two elements were diminished by approximately 80% at Lepanto. Cr (Puente Mayorga) and As (Campus and La Rabida) did not display relevant variations in the annual concentrations of PM10 in both periods.

3.4. Evolution of PM10 trace elements in year 2020

To study the influence of the Covid-19 mobility restrictions on the PM10 trace element concentrations, a more detailed study was performed during the year 2020. To this end, 2020 mean concentrations were compared to those obtained in the earlier period of 2013–2016. In both cases, the above-mentioned subperiods (pre-lockdown, lockdown, and relaxation) have been considered. The concentration variations are shown in Fig. 4.

The mean concentrations of V and Ni at the Puente Mayorga monitoring site showed significant differences during the three subperiods when comparing 2020 and 2013–2016. Even though the percentage reductions of both metals were approximately 80%, this decrease is

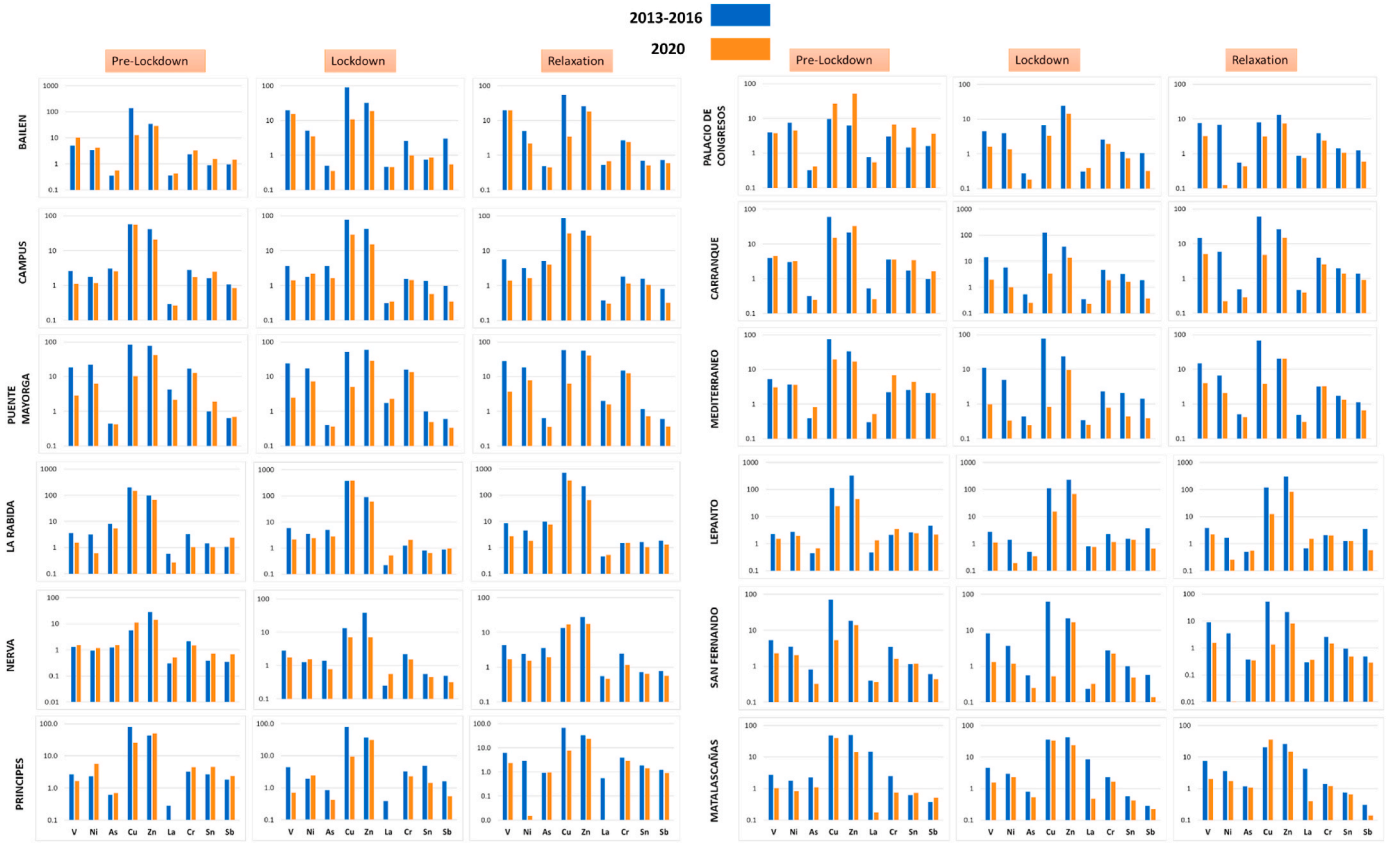

Fig. 4. Comparison between mean trace elements concentrations (ng m^{-3}) during 2020 and the period 2013–2016 taking into account the three different mobility periods: pre-lockdown, lockdown and relaxation.

related to the fuel change in the Algeciras Bay refinery and the inactivity of the nearby coal-fired power station since 2019. In addition, regarding La concentrations (cracking process catalysts of oil refinery) and Cr (stainless steel industry), no significant diminutions were observed in any subperiod. From these results, it can be inferred that the industrial activity developed in the area did not decrease during the lockdown.

A different scenario occurred at the industrial site of Bailen. V and Ni concentrations decreased during the lockdown and relaxation periods during 2020 with respect to 2013–2016 (Fig. 4). In this case, the high concentrations of Ni and V have been associated with the use of coke as fuel in brick factories; therefore, a lower demand for construction sector materials during the confinement may have produced a reduction in these emissions.

Concerning Cu and Zn concentrations derived from the Zn metallurgy activity at Lepanto, significant reductions were observed, between 70% and 90%, in the three subperiods. These activities do not seem to be affected by the confinement measures because the diminution concentrations were also maintained during the pre-lockdown and relaxation periods.

In the province of Huelva, Cu, Zn, and As concentrations showed the highest diminution in 2020 with respect to the 2013–2016 mean values in the lockdown and relaxation periods at Campus. This indicates a decrease in the emissions from the Cu-smelter previously defined. However, these toxic trace element concentrations did not show a high diminution during the lockdown at La Rabida, which is also affected by the Cu-smelter. The different scenarios given between La Rabida and Campus can result from fugitive emissions due to the handling of polymetallic sulphides in a port area close to La Rabida. (Millán-Martínez et al., 2021a).

Finally, significant reductions in Sn and Sb concentrations during the lockdown stage were higher than those observed in the pre-lockdown and relaxation periods. This decrease was registered in all the traffic monitoring sites as well as in urban and industrial stations such as San Fernando, Campus, and Puente Mayorga (Fig. 4). Traffic emissions were remarkably reduced by the imposed confinement in 2020.

The comparison of the PM10 trace element mean concentrations obtained in the three different subperiods in 2020 and 2013–2016 revealed the change in anthropogenic activities under mobility restrictions. Road traffic-related elements (mainly Sn and Sb) underwent a significant reduction during this period. In the industrial sector, the results showed that emissions from the stainless-steel factory (Cr) and the oil refinery (V, Ni, and La) in Puente Mayorga were maintained. Zn-smelters located in Lepanto were not affected during lockdown. Conversely, the ceramic industry in Bailen and the Cu-smelter affecting Campus (Huelva) experienced a decrease during confinement months.

4. Conclusions

Mobility restrictions imposed by the Spanish Government during the global pandemic of SARS-CoV-2 (Covid-19) gave rise to unprecedented conditions for evaluating the variation of certain air pollutant concentrations. In the present study, gaseous pollutants (NO_2 and SO_2) PM10 levels and trace element concentrations in PM10 during 2020 were compared to those obtained in 2013–2016 in Andalusia (Southern Spain). The results showed a strong decrease in NO_2 in the study area during the lockdown period resulting from traffic diminution. A smoother reduction was observed in PM10 levels, and a non-defined pattern was found for SO_2 levels.

The trace element results revealed an accused diminution of road traffic emissions during the lockdown period compared to previous years. Considering the elements derived from particular industrial emissions, different conditions can be distinguished. In Algeciras Bay, the concentration variations of Cr, V, and Ni, as well as the lack of reduction of SO_2 impacts during the lockdown period, corroborated the continuity of the industrial activity (oil refinery and stainless-steel factory) in the area. At the Bailen site, a significant decrease in elements derived from the brick production industry (Ni, V, Cu, Zn, and Pb) during the confinement period can be associated with a reduction in construction sector demand. In the city of Huelva, trace elements associated with Cu-smelter (As, Cu, and Zn) showed larger decreases during the lockdown and relaxation periods. This fact seems to be in concordance with the lower number of SO_2 impact days during March 2020, which points to a steady reduction in the Cu-smelter emissions.

The results obtained in this study are of great interest to air quality managers to determine the degree of reduction in the concentration of metals in ambient air during the confinement of the population. The most significant reduction in the metal concentration in PM10 is related to traffic mobility. However, metals derived from industry are dependent on the type of activity present.

Sample CRediT author statement

María Millán Martínez: Investigation, Writing – original draft. Daniel Sánchez-Rodas: Reviewing, Methodology. Ana M. Sánchez de la Campa: Reviewing, Methodology. Jesús D. de la Rosa: Funding acquisition, Reviewing.

Declaration of competing interest

The authors declare that they have no known competing financial interests or personal relationships that could have appeared to influence the work reported in this paper.

Acknowledgments

We would like to acknowledge the project of the Ministry of Science, Innovation and Universities of Spain (Project RTI2018-095937-B-I00), the co-financed project by the Andalusian Government and the EU (PY18-2332), and the Environmental Agency of Andalusia for financial and technical support. Funding for open access charge: Universidad de Huelva / CBUA.

Appendix A. Supplementary data

Supplementary data to this article can be found online at https://doi.org/10.1016/j.chemosphere.2022.134853.

References

Amato, F., Pandolfi, M., Escrig, A., Querol, X., Alastuey, A., Pey, J., Perez, N., Hopke, P. K., 2009. Quantifying road dust resuspension in urban environment by multilinear engine: a comparison with PMF2. Atmos. Environ. 43, 2770–2780. https://doi.org/10.1016/j.atmosenv.2009.02.039.

Amato, F., Alastuey, A., de la Rosa, J., González-Castanedo, Y., Sánchez de la Campa, A. M., Pandolfi, M., Lozano, A., Contreras González, J., Querol, X., 2014. Trends of road dust emissions contributions on ambient air particulate levels at rural, urban and industrial sites in Southern Spain. Atmos. Chem. Phys. https://doi.org/10.5194/acp-14-3533-2014.

Baldasano, J., 2020. COVID-19 lockdown effects on air quality by NO2 in the cities of Barcelona and Madrid (Spain). Sci. Total Environ. 741, 140353 https://doi.org/10.1016/j.scitotenv.2020.140353.

Bauwens, M., Compernolle, S., Stavrakou, T., Müller, J.F., van Gent, J., Eskes, H., Levelt, P.F., van der A, R., Veefkind, J.P., Vlietinck, J., Yu, H., Zehner, C., 2020. Impact of coronavirus outbreak on NO2 pollution assessed using TROPOMI andOMI observations. Geophys. Res. Lett. 47, e2020GL087978 https://doi.org/10.1029/2020GL087978.

Cachorro, V.E., Toledano, C., Prats, N., Sorribas, M., Mogo, S., Berjón, A., Torres, B., Rodrigo, R., de la Rosa, J., De Frutos, A.M., 2008. The strongest desert dust intrusion mixed with smoke over the Iberian Peninsula registered with Sun photometry. J. Geophys. Res. 113, D14S04 https://doi.org/10.1029/2007JD009582.

Ceballos-Santos, S., González-Pardo, J., Carslaw, D.C., Santurtún, A., Santibáñez, M., Fernández-Olmo, I., 2021. Meteorological normalisation using boosted regression trees to estimate the impact of COVID-19 restrictions on air quality levels. Int. J. Environ. Res. Publ. Health 18 (24), 13347. https://doi.org/10.3390/ijerph182413347.

CEPSA, 2020. Environmental Report. https://www.cepsa.com/stfls/corporativo/FICHEROS/declaracion-medioambiental-anexo-VII-la-rabida.pdf. last accessed 14 December 2021.

Chen, B., Stein, A.F., Castell, N., González-Castanedo, Y., de la Campa, A.M.S., de la Rosa, J.D., 2016. Modelling and evaluation of urban pollution events of atmospheric heavy metals from a large Cu-smelter. Sci. Total Environ. 539, 17–26. https://doi.org/10.1016/j.scitotenv.2015.08.117.

Chen, L.W.A., Chien, L.C., Li, Y., Lin, G., 2020. Nonuniform impacts of COVID-19 lockdown on air quality over the United States. Sci. Total Environ. 745, 141105 https://doi.org/10.1016/j.scitotenv.2020.141105.

Collivignarelli, M.C., Abba, A., Bertanza, G., Pedrazzani, R., Ricciardi, P., Miino, M.C., 2020. Lockdown for CoViD-2019 in Milan: what are the effects on air quality? Sci. Total Environ. 732, 139280 https://doi.org/10.1016/j.scitotenv.2020.139280.

de la Rosa, J.D., Sánchez de la Campa, A.M., Alastuey, A., Querol, X., González-Castanedo, Y., Fernández-Camacho, R., Stein, A.F., 2010. Using PM10 geochemical maps for defining the origin of atmospheric pollution in Andalusia (Southern Spain). Atmos. Environ. 44, 4595–4605. https://doi.org/10.1016/j.atmosenv.2010.08.009.

Donzelli, G., Cioni, L., Cancellieri, M., Llopis Morales, A., Morales Suárez-Varela, M.M., 2020. The effect of the covid-19 lockdown on air quality in three Italian medium-sized cities. Atmosphere 11, 1118. https://doi.org/10.3390/atmos11101118.

Donzelli, G., Cioni, L., Cancellieri, M., Llopis-Morales, A., Morales-Suarez-Varela, M., 2021. Relations between air quality and Covid-19 lockdown measures in Valencia, Spain. Int. J. Environ. Res. Publ. Health 18 (5), 2296. https://doi.org/10.3390/ijerph18052296.

EPER, 2019. Spanish Register of Emissions and Pollutant Sources. https://bit.ly/2BzRArN. last accessed 14 December 2021.

EPER, 2021. Spanish Register of Emissions and Pollutant Sources. https://bit.ly/2BzRArN. last accessed 14 December 2021.

European Commission, 2008. Directive 2008/50/CE on ambient air quality and cleaner air for Europe. Last Accesed July 2017. https://bit.ly/2R7Peu3.

Fernández-Camacho, R., de la Rosa, R., Sánchez de la Campa, A.M., González-Castanedo, Y., Alatuey, A., Querol, X., Rodríguez, S., 2010. Geochemical characterization of Cu-smelter emission plumes with impact in an urban area of SW Spain. Atmos. Res. 96, 590–601. https://doi.org/10.1016/j.atmosres.2010.01.008.

Fernández-Camacho, R., de la Rosa, J.D., Sánchez de la Campa, A.M., 2016. Trends and sources vs air mass origins in a major city in South-western Europe: implications for air quality management. Sci. Total Environ. 553, 305–315. https://doi.org/10.1016/j.scitotenv.2016.02.079.

Filonchyk, M., Hurynovich, V., Yan, H., 2021. Impact of covid-19 lockdown on air quality in the Poland, eastern Europe. Environ. Res., 110454 https://doi.org/10.1016/j.envres.2020.110454.

Hesterberg, T.W., Bunn, W.B., McClellan, R.O., Hamade, A.K., Long, C.M., Valberg, P.A., 2009. Critical review of the human data on short-term nitrogen dioxide (NO2) exposures: evidence for NO2 no-effect levels. Crit. Rev. Toxicol. 39 (9), 743–781. https://doi.org/10.3109/10408440903294945.

Higham, J.E., Ramirez, C.A., Green, M.A., Morse, A.P., 2021. UK COVID-19 lockdown: 100 days of air pollution reduction? Air Qual. Atmos. Health 14, 325–332. https://doi.org/10.1007/s11869-020-00937-0.

Kandari, R., Kumar, A., 2021. COVID-19 pandemic lockdown: effects on the air quality of South Asia. Environ. Sustain. 4, 543–549. https://doi.org/10.1007/s42398-020-00154-6.

Lijima, A., Sato, K., Yano, K., Tago, H., Kato, M., Kimura, H., Furuta, N., 2007. Particle size and composition distribution analysis of automotive brake abrasion dusts for the evaluation of antimony sources of airborne particulate matter. Atmos. Environ. 41 (23), 4908–4919. https://doi.org/10.1016/j.atmosenv.2007.02.005.

Mahato, S., Ghosh, K.G., 2020. Short-term exposure to ambient air quality of the most polluted Indian cities due to lockdown amid SARS-CoV-2. Sci. Total Environ. 188, 109835 https://doi.org/10.1016/j.scitotenv.2020.139086.

Martorell-Marugán, J., Villatoro-García, J.A., García-Moreno, A., Ĺopez-Domínguez, R., Requena, F., Merelo, J.J., Lacasãna, M., de Dios Luna, J., Díaz-Mochon, J.J., Lorente, J.A., Carmona-Śaez, P., 2021. DatAC: a visual analytics platform to explore climate and air quality indicators associated with the COVID-19 pandemic in Spain. Sci. Total Environ. 750, 141424 https://doi.org/10.1016/j.scitotenv.2020.141424.

Millán-Martínez, M., Sánchez-Rodas, D., Sánchez de la Campa, A.M., Alastuey, A., Querol, X., de la Rosa, J.D., 2021a. Source contribution and origin of PM10 and arsenic in a complex industrial region (Huelva, SW Spain). Environ. Pollut. 274, 116268–116278. https://doi.org/10.1016/j.envpol.2020.116268.

Millán-Martínez, M., Sánchez-Rodas, D., Sánchez de la Campa, A.M., de la Rosa, J.D., 2021b. Contribution of anthropogenic and natural sources in PM10 during North African dust events in Southern Europe. Environ. Pollut. 290, 118065 https://doi.org/10.1016/j.envpol.2021.118065.

MITECO, 2020. Spanish Ministry for the Ecological Transition and the Demographic Challenge. https://www.miteco.gob.es/es/calidad-y-evaluacion-ambiental/temas/atmosfera-y-calidad-del-aire/informeevaluacioncalidadaireespana2020_tcm30-529210.pdf. last acceesed 14 December 2021.

Moreno, T., Querol, X., Alastuey, A., Viana, M., Salvador, P., Sánchez de la Campa, A., Artiñano, B., de la Rosa, J., Gibbons, W., 2006. Variations in atmospheric PM trace metal content in Spanish towns: illustrating the chemical complexity of the inorganic urban aerosol cocktail. Atmos. Environ. 40, 6791–6803. https://doi.org/10.1016/j.atmosenv.2006.05.074.

Moreno, T., Querol, X., Alastuey, A., Gibbons, W., 2008. Identification of FCC refinery atmospheric pollution events using lanthanoid- and vanadium-bearing aerosols. Atmos. Environ. 42, 7851–7861. https://doi.org/10.1016/j.atmosenv.2008.07.013.

Naqvi, H.R., Mutreja, G., Shakeel, A., Siddiqui, M.A., 2021. Spatio-temporal analysis of air quality and its relationship with major COVID-19 hotspot places in India. Remote Sens. Appl. 22, 100473 https://doi.org/10.1016/j.rsase.2021.100473.

Pandolfi, M., González-Castanedo, Y., Alastuey, A., Rosa, J.d.l., Mantilla, E., Campa, A.S. d.l., Querol, X., Pey, J., Amato, F., Moreno, T., 2011. Source apportionment of PM10 and PM2.5 at multiple sites in the strait of Gibraltar by PMF: impact of shipping emissions. Environ. Sci. Pollut. Res. 18, 260–269. https://doi.org/10.1007/s11356-010-0373-4.

Querol, X., Alastuey, A., Pey, J., Pandolfi, M., Cusack, M., Pérez, N., Viana, M., Moreno, T., Mihalopoulos, N., Kallos, G., Kleanthous, S., 2009. African dust contributions to mean ambient PM10 mass-levels across the Mediterranean Basin. Atmos. Environ. 43 (28), 4266–4277. https://doi.org/10.1016/j.atmosenv.2009.06.013.

Querol, X., Alastuey, A., Rodriguez, S., Plana, F., Ruiz, C.R., Cots, N., Massague, G., Puig, O., 2001. PM10 and PM2.5 source apportionment in the Barcelona Metropolitan area, Catalonia, Spain. Atmos. Environ. 35, 6407–6419. https://doi.org/10.1016/S1352-2310(01)00361-2.

Querol, X., Alastuey, A., Viana, M., Rodríguez, S., Artíñano, B., Salvador, P., Garcia dos Santos, S., Fernández Patier, R., Ruiz, C.R., de la Rosa, J., Sánchez de la Campa, A. M., Menendez, M., Gil, J.I., 2004. Speciation and origin of PM10 and PM2.5 in Spain. J. Aerosol Sci. 35, 1151–1172. https://doi.org/10.1016/j.jaerosci.2004.04.002.

Querol, X., Alastuey, A., Moreno, T., Viana, M.M., Castillo, S., Pey, J., Rodríguez, S., Artiñano, B., Salvador, P., Sánchez, M., García Dos Santos, S., Herce Garraleta, M.D., Fernández-Partier, R., Moreno-Grau, S., Negral, L., Minguillón, M.C., Monfort, E., Sanz, M.J., Palomo-Marín, R., Pinilla-Gil, E., Cuevas, E., de la Rosa, J., Sánchez de la Campa, A.M., 2008. Spatial and temporal variations in airborne particulate matter (PM10 and PM2.5) across Spain 1999–2005. Atmos. Environ. 42, 3964–3979. https://doi.org/10.1016/j.atmosenv.2006.10.071.

Querol, X., Massagué, J., Alastuey, A., Moreno, T., Gangoiti, G., Mantilla, E., Duéguez, J. J., Escudero, M., Monfort, E., Pérez García-Pando, C., Petetin, H., Jorba, O., Vázquez, V., de la Rosa, J., Campos, A., Muñóz, M., Monge, S., Hervás, M., Javato, R., Cornide, M.J., 2021. Lessons from the COVID-19 air pollution decrease in Spain: now what? Sci. Total Environ. 779, 146380 https://doi.org/10.1016/j.scitotenv.2021.146380.

Rodríguez, S., Querol, X., Alastuey, A., Kallos, G., Kakaliagou, O., 2001. Saharan dust contributions to PM10 and TSP levels in Southern and Eastern Spain. Atmos. Environ. 35, 2433–2447. https://doi.org/10.1016/S1352-2310(00)00496-9.

Salvador, P., Artíñano, B., Molero, F., Viana, M., Pey, J., Alastuey, A., Querol, X., 2013. African dust contribution to ambient aerosol levels across central Spain: characterization of long-range transport episodes of desert dust. Atmos. Res. 127, 117–129. https://doi.org/10.1016/j.atmosres.2011.12.011.

Sánchez de la Campa, A.M., de la Rosa, J.D., 2014. Implications for air quality and the impact of financial and economic crisis in South Spain: geochemical evolution of atmospheric aerosol in the ceramic region of Bailén. Atmos. Environ. 98, 519–529. https://doi.org/10.1016/j.atmosenv.2014.09.023.

Sánchez de la Campa, A.M., de la Rosa, J.D., González-Castanedo, Y., Fernández-Camacho, R., Alastuey, A., Querol, X., Pio, C., 2010. High concentrations of heavy metals in PM from ceramic factories of Southern Spain. Atmos. Res. 96, 633–644. https://doi.org/10.1016/j.atmosres.2010.02.011.

Sánchez de la Campa, A.M., Sánchez-Rodas, D., Alsioufi, L., Alastuey, A., Querol, X., Jesús, D., 2018. Air quality trends in an industrialised area of SW Spain. J. Clean. Prod. 186, 465–474. https://doi.org/10.1016/j.jclepro.2018.03.122.

Sánchez de la Campa, A.M., Sánchez-Rodas, D., Márquez, G., Romero, E., de la Rosa, J. D., 2020. 2009–2017 trends of PM10 in the legendary Riotinto mining district of SW Spain. Atmos. Res. 238, 104878 https://doi.org/10.1016/j.atmosres.2020.104878.

Sánchez-Rodas, S., Alsioufi, L., Sánchez De La Campa, A.M., González-Castanedo, Y., 2017. Antimony speciation as geochemical tracer for anthropogenic emissions of atmospheric particulate matter. J. Hazard Mater. 324, 213–220. https://doi.org/10.1016/j.jhazmat.2016.10.051.

Santurtún, A., Sánchez-Lorenzo, A., Villar, A., Riancho, J.A., Zarrabeitia, M.T., 2017. The in-fluence of nitrogen dioxide on arrhythmias in Spain and its relationship with atmospheric circulation. Cardiovasc. Toxicol. 17, 88–96. https://doi.org/10.1007/s12012-016-9359-x.

Shakoor, A., Chen, X., Farooq, T.H., 2020. Fluctuations in environmental pollutants and air quality during the lockdown in the USA and China: two sides of COVID-19 pandemic. Air Qual. Atmos. Health. https://doi.org/10.1007/s11869-020-00888-6.

Shi, X., Brasseur, G.P., 2020. The response in air quality to the reduction of Chinese economic activities during the covid-19 outbreak. Geophys. Res. Lett. 47, e2020GL088070 https://doi.org/10.1029/2020GL088070.

Silver, B., He, X., Arnold, S.R., Spracklen, D.V., 2020. The impact of COVID-19 control measures on air quality in China. Environ. Res. Lett. 15, 084021 https://doi.org/10.1088/1748-9326/aba3a2.

Stein, A.F., Draxler, R.R., Rolph, G.D., Stunder, B.J.B., Cohen, M.D., Ngan, F., 2015. NOAA's HYSPLIT atmospheric transport and dispersion modelling system. Bull. Am. Meteorol. Soc. 96, 2059–2077. https://doi.org/10.1175/BAMS-D-14-00110.1.

Tobías, A., Carnerero, C., Reche, C., Massagué, J., Via, M., Minguillón, M.C., Alastuey, A., Querol, X., 2020. Changes in air quality during the lockdown in Barcelona (Spain) one month into the SARS-CoV-2 epidemic. Sci. Total Environ. 726, 138540 https://doi.org/10.1016/j.scitotenv.2020.138540.

Viana, M., Querol, X., Alastuey, A., Cuevas, E., Rodríguez, S., 2002. Influence of African dust on the levels of atmospheric particulates in the Canary Islands air quality network. Atmos. Environ. 36, 5751–5875. https://doi.org/10.1016/S1352-2310(02)00463-6.

von Uexküll, O., Skerfving, S., Doyle, R., Braungart, M., 2005. Antimony in brake pads-a carcinogenic component? J. Clean. Prod. 13, 19–31. https://doi.org/10.1016/j.jclepro.2003.10.008.

Wang, J., Du, G., 2020. COVID-19 may transmit through aerosol. Ir. J. Med. Sci. 1971, 1–2. https://doi.org/10.1007/s11845-020-02218-2.

World Health Organization, 2020a. Coronavirus Disease (COVID-19) Outbreak. Available from: who.int/emergencies/diseases/novel-coronavirus-2019, (Last accessed in 10 December 2021).

World Health Organization, 2020b. Novel Coronavirus (2019-nCov), Situation Report-147, 15 June 2020. https://www.who.int/docs/default-source/coronaviruse/situation-reports/20200615-covid-19-sitrep-147.pdf (Last accessed in 10 December 2021).

Wu, X., Nethery, R.C., Sabath, B.M., Braun, D., Dominici, F., 2020. Exposure to Air Pollution and COVID-19 Mortality in the United States: a Nationwide Cross-Sectional Study. medRxiv. https://doi.org/10.1101/2020.04.05.20054502.

Wyche, K.P., Nichols, M., Parfitt, H., Beckett, P., Gregg, D.J., Smallbone, K.L., Monks, P. S., 2021. Changes in ambient air quality and atmospheric composition and reactivity in the South East of the UK as a result of the COVID-19 lockdown. Sci. Total Environ. 755, 142526 https://doi.org/10.1016/j.scitotenv.2020.142526.

Xu, K., Cui, K., Young, L.H., Hsieh, Y.K., Wang, Y.F., Zhang, J., Wan, S., 2020. Impact of the COVID-19 event on air quality in central China. Aerosol Air Qual. Res. 20, 915–929. https://doi.org/10.4209/aaqr.2020.04.0150.

Zhu, Y., Xie, J., Huang, F., Cao, L., 2020. Association between short-term exposure to air pollution and COVID-19 infection: evidence from China. Sci. Total Environ. 727, 138704 https://doi.org/10.1016/j.scitotenv.2020.138704.